UV-triggered Transient Electrospun Fiber Mats from Poly(Propylene Carbonate)/Poly(Phthalaldehyde) Polymer Blends

A Thesis

Presented to the Faculty of the Graduate School

of Cornell University

In Partial Fulfillment of the Requirements for the Degree of

Master of Science

by

Chengjian Shi

August.2018

ABSTRACT

Low-ceiling temperature polymers with triggered transience have gained attention due to their potential applications in multiple fields, ranging from lithography to decomposable packaging, as well as for channel manufacturing in microfluidic devices. Besides the development of novel transient materials, advanced electrospinning techniques have also been utilized to increase a materials surface area, which can result in a faster decomposition rate. Thus, it would be of interest to explore the unique characterization of electrospun transient fiber mats made of low-ceiling temperature polymers and their potential usage as support substrate for microelectronic devices.

This work reports the first transient electrospun nanofiber mat triggered by UV-irradiation using poly(propylene carbonate) (PPC)/poly(phthalaldehyde) (cPPA) polymer blends. The ability to trigger room temperature transience in nanofibers mats without the need for additional heat or solvent expands its utility in non-biological fields, especially for transient electronic devices. The addition of a photoacid-generator (PAG) to the system working in combination with UV light provides an acid source to enhance degradation since both polymer backbones are acid-sensitive. Electrospinning enables the production of PPC/cPPA composite nanofiber mats capable significant degradation upon exposure to UV radiation while maintaining relatively high mechanical properties. An acid amplifier (AA), an auto-catalytically decomposing compound triggered by acid, was used to generate more acid and accelerate nanofiber degradation. The electrospun fiber mats can be post-annealed to achieve an improved mat mechanical strength of ~ 170 MPa.

BIOGRAPHICAL SKETCH

Chengjian Shi completed his undergraduate study in Materials Science and Engineering at Zhejiang University, China in July 2016. Then he became a MS student majoring in Materials Science and Engineering at Cornell University starting from August 2016 until the present. During this period, he worked under the guidance of Prof. Christopher K. Ober researching electrospun transient polymer fiber mats for his MS thesis. After finishing his MS degree, Chengjian will continue his graduate career as a PhD candidate at the Institute of Molecular Engineering in the University of Chicago starting in October 2018.

ACKNOWLEDGMENTS

First, I would like to thank Prof. Ober for his kindness and guidance to my academic research within the past two years at Cornell University. I feel lucky to have Prof. Ober as my PI as he has had a positive influence over me as both a critical scientist as well as a mentor. In addition, I would also like to thank other members in Prof. Ober's group who have offered me great help during my study at Cornell University. I want to thank Dr. Peter Ohlendorf for teaching me the fundamentals of electrospinning, propelling my skills in it as well as characterization techniques needed to further my research. Without his expertise I would not have been able to finish the project independently. I also want to thank Yiren Zhang and Hong Xu for being good consultants whenever I faced problems on chemical synthesis. Furthermore, I really appreciate the kindness and friendship that I have received from all group members in the past two years. In the end, I want to send my best to my parents, who always support me and love me in my life.

Table of Contents

Chapter 1

1.1 Background

1.1.1 Introduction to depolymerizable polymers

Depolymerizable polymers, also known as stimuli-responsive polymers, with their close relationship to self-immolative polymers have gained significant attention in recent years due to their potential usage in a wide range of fields. Stimuli-responsive polymers are capable of depolymerization when response to external stimuli then generates separate monomers.[1] To be clear, it must be mentioned that we define polymers that can degrade to monomer with no difference from the parent monomer as depolymerizable polymers while those that simply fragment to small segments are self-immolative polymers.[2] For either case, their development is largely concentrated in low-ceiling temperature (T_c) polymers and several mechanisms have been established to explain the initiation of the unzipping sequence of polymer backbones.

First, a brief introduction to the fundamental concept of polymers ceiling-temperatures (T_c) will be given.[3] The basic idea of T_c depends on the thermal equilibrium temperature of polymerization reaction, as shown in scheme 1.1 below. The radical polymerization process (Equation 1) in most cases are exothermic and exoentropic (both ΔH and ΔS below 0), therefore the polymerization free energy ΔG_p can inherently reach thermal equilibrium ($\Delta G_p=0$) at a certain critical temperature (Equation 2) and above which the whole reaction could be reversed (ΔG_p above 0). This critical temperature is defined as ceiling-temperature, where the rate of polymerization is equivalent to the rate of depolymerization (Equation 3, 4), and the measurement of monomer concentration variation can enable us to determine T_c accurately (Equation 5) as shown in Figure 1.1.[4,5] A

comprehensive understanding of T_c inspires us that by using sufficiently low-T_c polymers, the inherently unstable backbone chain bond could be cleaved under mild conditions.

Then we need to discuss mechanisms to trigger the depolymerization process of typical low-T_c

$$\mathrm{M} + A_n \cdot \underset{Kd}{\overset{Kp}{\rightleftarrows}} A_{n+1} \cdot \qquad (1)$$

$$\Delta G_p = \Delta H_p - T\Delta S_p \qquad (2)$$

$$\Delta H_p - T_C \Delta S_p = 0 \qquad (3)$$

$$T_c = \frac{\Delta H_p}{\Delta S_p} \qquad (4)$$

$$\ln[M] = \frac{\Delta H_p}{\mathrm{R}} \left(\frac{1}{T}\right) - \frac{\Delta S_p}{\mathrm{R}} \qquad (5)$$

Scheme 1.1. Classic radical polymerization reaction and derivative of T_c

polymers.[6] Since the unstable nature of low-T_c polymers requires "capping" at the end of the

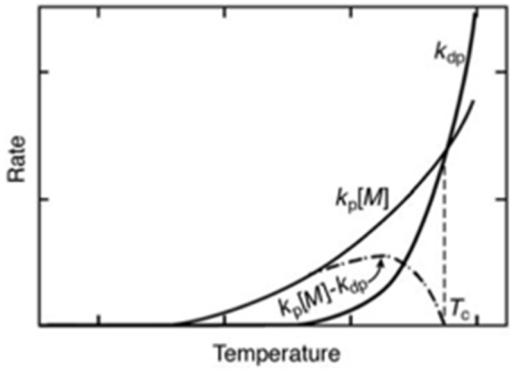

Figure 1.1. Polymerization and depolymerization rate as a function of temperature. [5]

backbone to protect the free radical, hence the intuitive method to initiate depolymerization of the polymer chain uses external stimuli to cleave the "end-cap" and release a free radical. As illustrated in Figure 1.2, the synthetic process of poly(benzyl carbamate) is a step-growth propagation mechanism and quenched polymerization by end-cap group.[7] Then depolymerization is triggered by external stimuli and the free radical is exposed due to end-cap cleavage, which leads to

monomer regeneration. This depolymerization mechanism is known as end-chain scission or "unzipping".[8] Besides the end-chain scission mechanism, which predominately occurs on polymers stabilized with a stimuli responsive end-cap, there is another depolymerization mechanism called random-chain scission or "chain-shattering".[9] Other than depropagation from a chain end, a stimulus triggered group is functionalized on the random-chain scission polymer backbone. For instance, in a UV-triggered depolymerization process is shown in Figure 1.3, the functionalized UV-responsive group on the side chain, when exposed to UV irradiation, initiates depolymerization through an amine base and further heat-treatment causes a subsequent depolymerization process.[10] The future development of depolymerizable polymers will concentrate on functional stimuli-responsive groups on the backbone that can be triggered by single stimuli and lead to direct depolymerization.

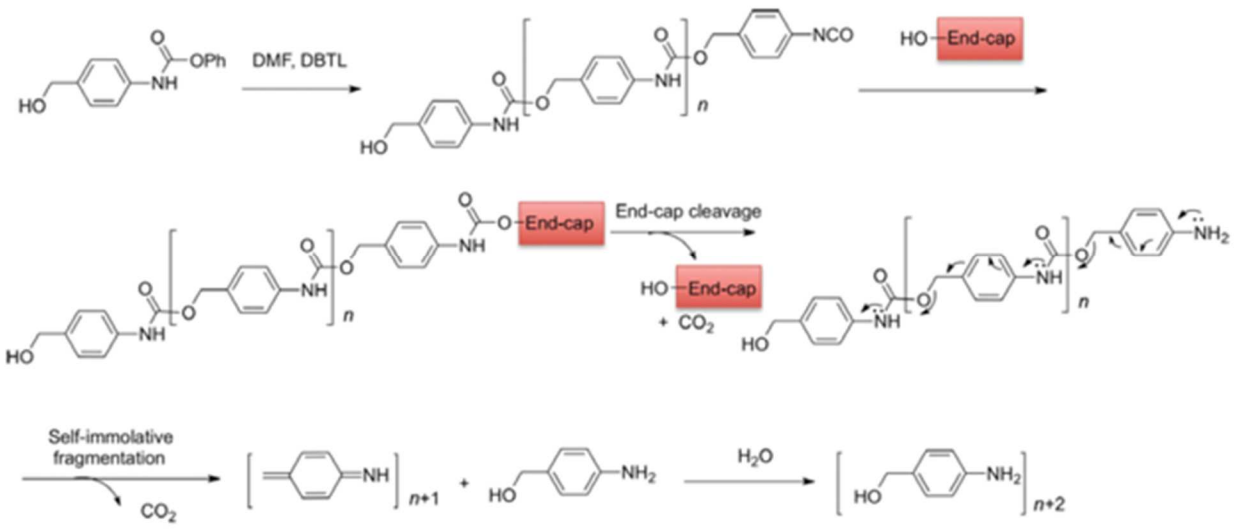

Figure 1.2. Polymerization of poly(benzyl carbamate) and its depolymerization process following end-cap cleavage. [7]

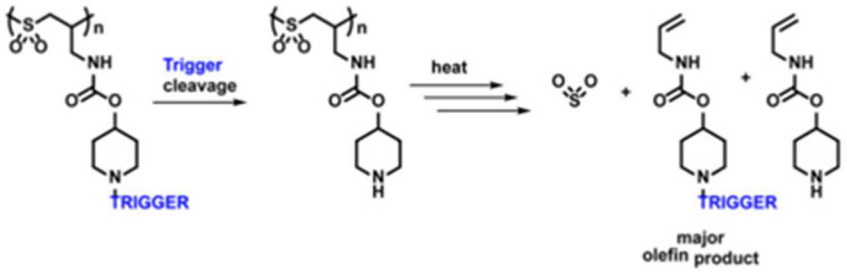

Figure 1.3. Chain shattering depolymerization triggered by UV-irradiation. [10]

1.1.2 Introduction to stimuli-responsive polymer applications

1.1.2.1 Photolithography

One of the original purposes of studying depolymerizable polymers was for photolithography applications, the effective depolymerization mechanism to degrade polymer into monomer with solubility changes of interest for lithography.[2] Electron beam lithography, for instance, has been developed to fabricate microelectronic devices through delineation of conducting and insulating materials into specific patterns.[11] In a lithographic step a substrate to support pattern delineation is covered with a depolymerizable polymeric film. In this field, a polymer such as poly(methyl methacrylate) (PMMA) is known as a suitable photoresist polymer capable of degrainge under electron beam irradiation, but its low photosensitivity limits its industrial fabrication on a large scale.[12] To compensate for the limitations of PMMA, poly(olefin sulfone)s have been introduced due to their high photosensitivity under high energy irradiation.[13] After extensive exploration of poly(olefin sulfone)s as candidates for photo-resist materials, poly(1-butene sulfone) has been largely commercialized because of its excellent properties such as rapid depolymerization rate and ideal film characterization. Besides that, the potential usages of low-T_c poly(phthalaldehyde) combined with photoacid generator as a polymeric photoresist film has been investigated as well due to its straightfoward synthesis procedure and solubility in commonly used organic solvents.

1.1.2.2 Triggered release

Stimuli-responsive polymerizable polymers are ubiquitous capsule materials to control the release of preserved contents in multiple fields include self-healing materials, nutrient preservation, drug delivery, etc. Triggering methods are different regarding its specific application, so a variety of stimuli have been developed to release contents accordingly, as shown in Figure 1.4.[14] In this paper, we only give a brief introduction of stimuli-responsive drug release polymer capsules via end-cap cleavage depolymerization.

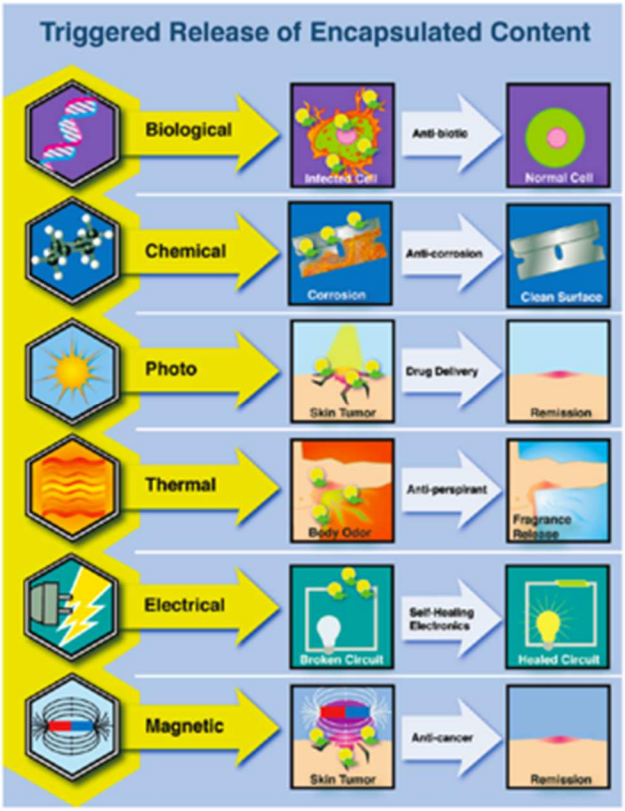

Figure 1.4. Multiple stimuli-triggering mechanisms for depolymerizable polymer microcapsules. [14]

As illustrated above, end-capped depolymerizable polymers can be easily triggered to initiate end-chain scission by external stimuli such as light, pH, chemistry, etc. The end-caps provide essential potential capability to amplify the signal of low-concentration stimulus. Poly(ethyl glyoxylate) (PEtG), a low-T_c polymer, has been reported by Gillies and co-workers as a self-immolative polymer because the low toxicity depolymerized products make PEtG a promising material as encapsulant for drug delivery.[15] Furthermore, a UV light-responsive block co-polymer composed of PEtG and poly(ethylene oxide) (PEO) has been developed, and the triggered depolymerization of micellar nanoparticles formed by PEtG-PEO copolymer was achieved through photolysis of PEtG to initiate an unzipping process and release its contents using a decomposition progress as shown in Figure 1.5.

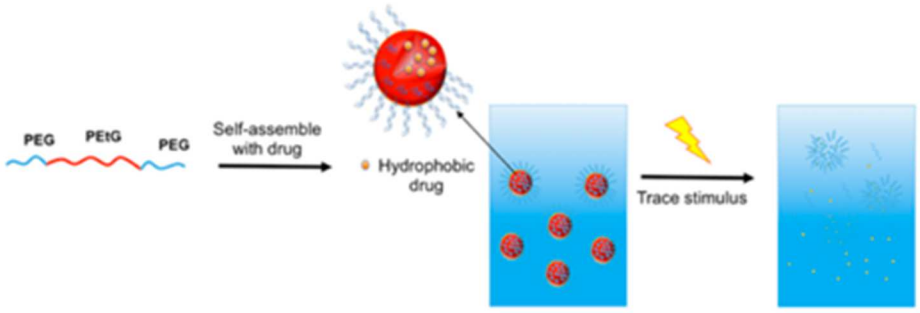

Figure 1.5. UV-light triggering mechanism of PEtG-PEO microcapsule drug delivery. [15]

1.1.2.3 Transient substrate and template materials

Applying depolymerizable polymers into transient substrates and template materials is a growing interest in recent research compared to permanent stable structure materials.[16] One of the essential uses of a depolymerizable polymers is for fabrication of temporary holders for mechanical and electrical devices taking advantage of the rapid stimuli-responsive change of polymers into low molecular weight monomer that can form a gas cavity or air gap in an encapsulation layer. Here

in this paper, we introduce poly(propylene carbonate) (PPC) utilization as a sacrificial polymer to

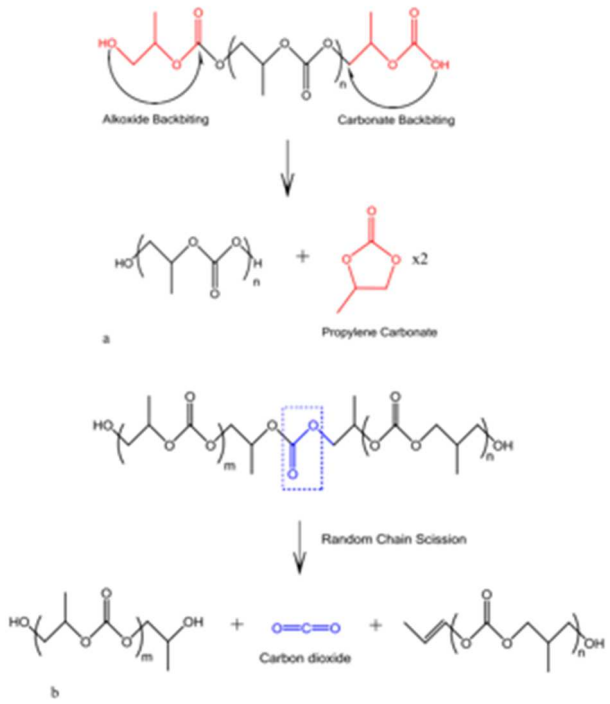

Figure 1.6. a. Unzipping process of PPC occurs at lower temperature. b. Random chain scission process dominates at higher temperature. [16]

fabricate air-gap microelectronic devices due to its excellent thermal decomposition properties.[17] Thermal decomposition of PPC involves two mechanisms as we have discussed in the section above, random chain scission takes place at higher temperature while unzipping predominates at lower temperature because the activation energy of chain scission is higher than unzipping process in thermal decomposition as shown in Figure 1.6. Studies of PPC have successfully expanded the onset depolymerization temperature of PPC in a wide temperature window from 70°C to 260°C (e.g., 5% weight loss temperature), so it can be applied in various applications. Also the low molecular weight products of propylene carbonate and carbon dioxide can escape most encapsulation layers to fabricate air-gaps effectively. The microelectronic patterning process with PPC is illustrated in Figure 1.7, where a photo-acid-generator (PAG) or photo-base-generator

(PBG) was incorporated into the PPC solution and spin-cast on a substrate to make a photo-sensitive PPC layer, then both UV-irradiation and thermal treatment were applied to initiate the PPC depolymerization.

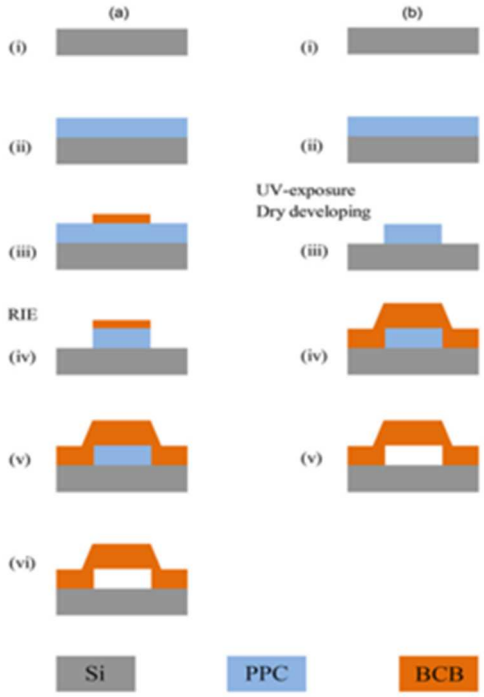

Figure 1.7. Air-gap fabrication from PPC layer through two different patterning techniques. a. Reactive ion-etching (RIE). b. Direct photo-patterning process. [17]

Besides the application of PPC for microelectronic devices, it's also important to introduce poly(phthalaldehyde) (PPA) as a transient substrate material for transient microelectronic devices. Jeffery Moore and co-workers have found a cyclic-structure PPA (cPPA) different from the traditional end-capped linear structure PPA.[18] This novel polymer structure has shown higher stability in storage without the concern of a non-volatile end-capping group, thus it has been further employed as substrate support for transient microelectronic devices. As shown in Figure 1.8, when incorporated with PAG, this low-T_c polymer with acid-sensitive backbone has excellent decomposition properties triggered solely by UV-irradiation.

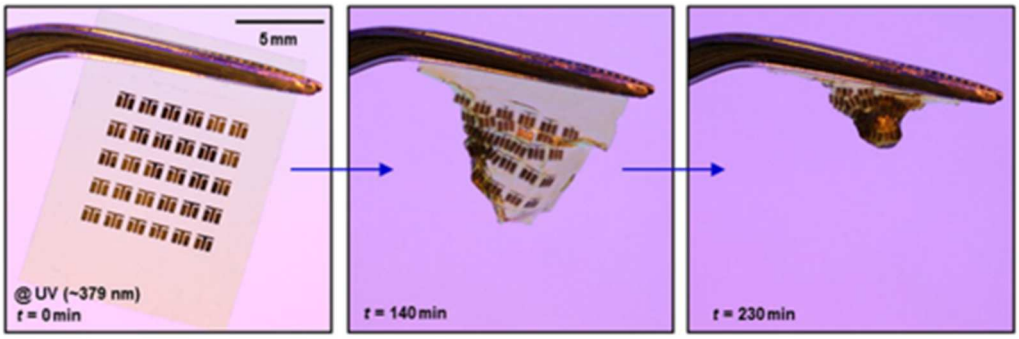

Figure 1.8. Triggered depolymerization of cPPA films as microelectronic substrate. Films are embedded with PAG such that UV-irradiation initiates acid-catalyzed depolymerization of substrate follower by electronic destruction. [18]

1.1.3 Introduction to electrospinning

Electrospinning, also known as electrostatic spinning, has been developed as a versatile technique to produce ultrathin fibers from a variety of polymers and composite materials.[19] The straightforward electrospinning process in large scale production ensures its potential usage in a wide range of fields include tissue engineering and drug delivery that cross-link with potential applications of depolymerizable polymer materials.[20] The another advantage to utilize electrospinning method to the field of depolymerizable polymer materials is the unique morphology of fiber formation, as a result of large surface area ratio of fiber mat, the response rate of stimuli-responsive polymers to external stimuli is therefore largely increased.[21]

To begin with, it's necessary that we briefly introduce the mechanism of electrospinning. A typical electrospinning set-up is shown in Figure 1.9, the conductive solution ejected from a syringe to collector via extremely high voltage difference in the gap (from 5 ~ 50 kV), meanwhile, the spinning process vaporizes solvent and continuously deposits polymer fibers on the collector.[22] The characteristics of collected fibers can be easily modulated by changing the electrospinning set-up parameters (solution concentration, applied voltage, flow rate, solvent conductivity,

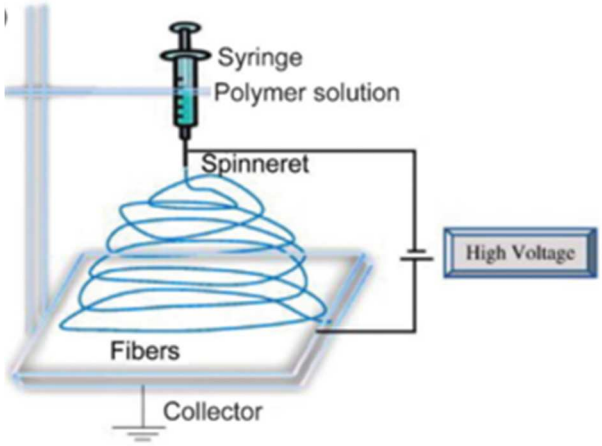

Figure 1.9. Vertical electrospinning set-up. [20]

distance between syringe and collector, etc.). For example, by slightly increasing the applied voltage and flow rate, we can dramatically change the morphology of fibers with decreased fiber diameter. In addition, we can also acquire highly oriented fibers by alternating the collector plate by rotating the collector or using a co-axial syringe to produce core-shell structured fibers. The variation in morphology made possible by the electrospinning method guarantees that depolymerizable polymers are available for various fields.

As we know, the degradation of stimuli-responsive polymers is highly dependent on the stimulus transfer rate to the material, thus the unique morphology properties of electrospinning nanofibers can boost the materials response time to a variety of stimuli (pH, temperature, photo, protein, gas, etc.).[23] The extremely high surface area and porous structure of electrospun fibers is beneficial for controlling the degradation rate of stimuli-responsive polymers. For instance, Ober and co-workers have recently reported transient fiber mats of electrospun PPC composite with remarkable mechanical properties.[24] As shown in Figure 1.10, the high surface ratio porous PPC composite fiber mats were investigated to achieve exceptional low thermal decomposition temperature and high mechanical properties by incorporating small amounts of PAG and nano-clay in the electrospinning solution. Furthermore, post-annealing techniques were later applied to the

electrospun fiber mats below the onset decomposition temperature to largely increase the Young's modulus from 54.5 MPa to 746.8 MPa, which is a typical technique to optimize the mechanical properties of fiber mats.

1.2 Motivation and goal

The goal of this MS project has been to develop a UV-sensitive decomposable material that will

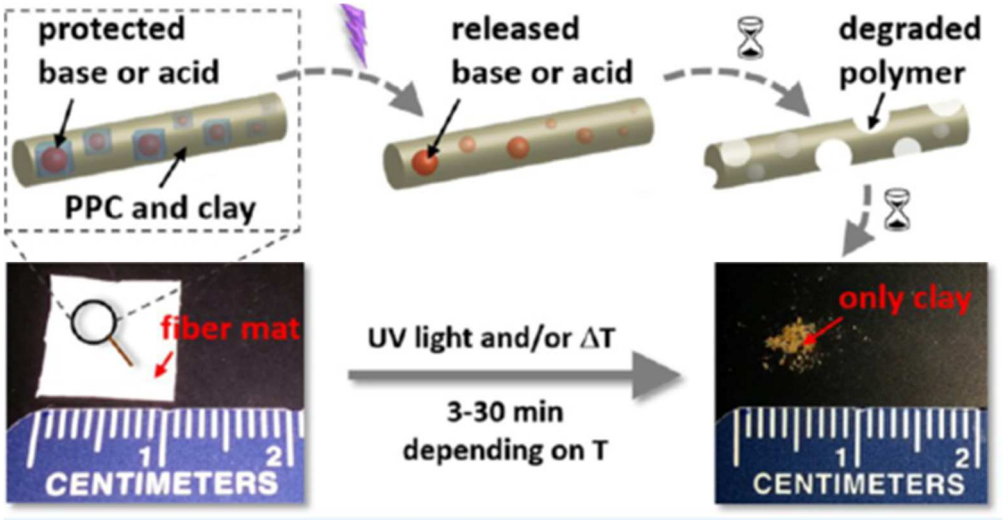

Figure 1.10. Decomposition scheme of electrospun PPC composite fiber mat under UV irradiation. [24]

vanish under mild conditions as a transient rigid support for microelectronic devices. To satisfy the goals of our projects, based on the information above, low-T_c stimuli-responsive polymers have been considered as ideal materials to meet the requirements due to their highly controllable stimulus selection and rapid depolymerization process. The specific choice of stimuli-responsive polymer candidates will be comprehensively explained in the following chapter. In addition, electrospinning methods have been applied to further increase the degradation and mechanical properties of depolymerizable polymers.

Chapter 2

2.1 Background and motivation

As we have discussed above, depolymerizable polymers are typically low ceiling temperature polymers, which can respond to specific external stimuli have garnered significant interest in recent years due to their potential use in a variety of fields,[2] such as triggered release capsules,[22] transient electronic packaging,[18, 12] photoresist materials in lithography,[25] molecular amplifiers[6, 26] and self-healing composite materials.[27, 28] The triggering stimuli varies depending on a particular application, including mechanical force,[29, 30] chemical change,[14] biological effect,[31] thermal treatment[32, 33] and UV irradiation.[34] However, the majority of researchers have accomplished transience by submerging substrates into biofluid or aqueous solutions and making use of hydrolysis or enzymatic degradation. This triggering strategy limits their usage in non-biological applications.[35] UV-triggers are an appealing agent in applications for release of microcapsule content with advantages of remotely applying precisely controlled irradiation intensity and exposure time, avoiding addition of external solvents or solutions,[36] which is important for solid state applications.[35] In this report, we focus our discussion on the use of UV irradiation as external stimulus. Several fabrication techniques have been utilized to process transient polymers in various morphologies for different usages.

Electrospinning is a highly versatile technique[23, 24] with the ability to efficiently produce non-woven continuous fibers and control network micro-morphology in a straightforward manner. The resulting product has extremely high surface to volume ratio, which permits faster decomposition speed with stimuli-responsive polymers[25] in contrast to a traditional high density product. Stimuli-responsive electrospun fibers are attractive in a wide range of applications including drug delivery microcapsule production,[25] transient filter applications,[26] as sacrificial template[27] and in tissue

engineering,[28] Our previous investigation[26] showed for the first time that electrospun poly(propylene carbonate) (PPC) composite fiber mats decompose in response to combined UV and thermal treatment. However, high temperature thermal treatment is commonly an unfavorable approach to remotely trigger transient microelectronic device fabrication, since substantial power may be required.[29] Poly(phthalaldehyde) (PPA) was first reported in 1967 then subsequently developed as a stimuli-responsive polymer in multiple fields due to its low ceiling temperature (~ - 40 °C) and easily modulated end groups.[30, 31] Joshua et al. created cyclic-poly(phthalaldehyde) (cPPA), which proved to be more stable under storage conditions and eliminated the concern of non-volatile end group residue, to improve its applicability as transient electronic device packaging.[32] Nevertheless, the relatively poor mechanical properties including the brittleness of cPPA limit its applications.

These findings inspired us to explore the possibility of combining PPC and cPPA through electrospinning techniques to optimize the properties of both. Electrospun polymer blends have been widely explored in tissue engineering as biodegradable scaffolds, as the unique synergistic degradation and mechanical properties of electrospun polymer blends fulfill the requirements to support cell growth.[42, 43] Here, we demonstrate a new transient electrospun fiber mat, which requires only UV radiation exposure for full decomposition, while also initially possessing relatively high mechanical properties compared to other degradable fiber mats. Firstly, we characterize electrospun PPC/cPPA composite fiber mat in various compositions. Because the backbones of both polymers are acid sensitive, a photo-acid-generator (PAG) was selected in a fixed weight ratio compared to the polymer blend. Furthermore, 3-hydroxy-3-methylbutyl 4-(trifluoromethyl)benzenesulfonate (acid amplifier, AA), a compound normally used in EUV lithography that decomposes auto-catalytically in the presence of acid to generate more acid,[44, 45]

was employed to optimize the degradation of the polymer blends. Post-annealing processes under controlled temperature conditions during manufacture have been demonstrated as an effective method to increase the strength of the fiber mat.[46]

2.2 Experimental section

2.2.1 Ingredients and materials synthesis

All materials were used as received unless otherwise noted. Poly(propylene carbonate) (**PPC**, MW~130.000 Da, Novomer), N-hydroxynaphthalimide triflate (**PAG**, >99%, Sigma-Aldrich), dichloromethane (**DCM,** extra dry, 99.9 %, AcroSeal), pyridine (extra dry, 99.5 %, AcroSeal), boron trifluoride diethyl etherate (**$BF_3 \cdot OEt_2$**, ≥46.5 %, Aldrich), 3-methyl-1,3-butanediol (>98.0 %, TCI), 4- (Trifluorormethyl)benzenesulfonyl chloride (97 %, Sigma-Aldrich). *o*-phthalaldehyde (***o*-PA,** 98.0 %**,** Alfa-Aesar) was purified through hot filtration at the boiling temperature in DCM solution then recrystallized twice in DCM/hexane solution according to a literature procedure.

Synthesis of cPPA. The cyclic-polyphthalaldehyde (**cPPA**) was synthesized following a literature procedure[41] with minor modification. Recrystallized *o*-PA (3.0 g, 22.5 mmol) was cooled to -78 °C in a solution of dry DCM (30 mL), freeze pump thawed three times, then $BF3 \cdot OEt_2$ (0.06 mL, 0.48 mmol) was injected to the solution as initiator. After two hours of polymerization under strong stirring conditions, pyridine (0.36 mL, 4.5 mmol) was added to quench the reaction by stirring for two hours. The final product was brought to room temperature then precipitated by pouring into methanol. Further purification was conducted by re-dissolving into DCM and re-precipitating into methanol at least two times. The final product was characterized by

^{1}H NMR spectra. ^{1}H NMR (400MHz, DMSO) δ 7.43 ppm (br, 4H, J = 4.00Hz),δ 6.65 ppm (br, 2H, J = 2.11Hz).

Polymer	Yield (%)	M_n (KDa)	PDI
cPPA	80	49	1.61

Synthesis of Acid Amplifier (AA). The 3-hydroxy-3-methylbutyl 4-(trifluoromethyl) benzenesulfonate (**Acid Amplifier**) was synthesized following a literature procedure. 4-(Trifluoromethyl) benzenesulfonyl chloride (5.63 g, 23 mmol) was added to a solution of 3-methyl-1,3-butanediol (2.92 g, 27.9 mmol) in pyridine (23 mL). The mixed solution was stirred at 0 °C for two hours then diluted with ethyl acetate (40 mL) and washed with HCl (3 x 50 mL). Saturated aqueous $NaHCO_3$ (50 mL) and NaCl (50 mL) were used to neutralize the solution. Then the organics were dried over Na_2SO_4 and concentrated to get the final product (5.3 g, 62 %). The product was characterized by ^{1}H NMR spectroscopy ^{1}H NMR (400MHz, $CDCl_3$) δ 8.06 ppm (d, 2H, J = 0.96 Hz), δ 7.84 ppm (d, 2H, J = 0.99 Hz), δ 4.29 ppm (t, 2H, J = 0.97 Hz) δ 1.90 ppm (t, 2H, J = 1.0 Hz), δ 1.24 (s, 6H, J = 3.08 Hz).

2.2.2 Electrospinning set-up

Spinning Solution Preparation. Based on our previous investigation, for 10 wt% PPC, relative to solvent, the optimum electrospinning solvent composition was dichloromethane (**DCM**)/dimethylformamide (**DMF**) with 80/20 vol%. In this research, the solutions of mixed PPC, cPPA, PAG, AA were prepared under yellow light in an aluminum foil covered glass vial. For the

precise composition, please see Table 1 (the subscript of polymer blends in Table 1 are PPC/cPPA weight ratio and PAG/AA shows in wt% are relative to polymer blends). The weight percent of polymer blend to the entire solution was 10 wt%, and solutions was shaken overnight to ensure homogeneous mixtures for continuous electrospinning conditions.

Electrospinning Setup. The electrospinning was performed in a horizontal Spraybase electrospinning setup as shown in Scheme 2.1. Solutions were spun through a needle (inner diameter = 0.6mm) and collected on a stainless steel flat plate collector covered by parchment paper with graphite on the surface. For each solution composition according to Table 2.1, a constant total volume of 6 mL solution was electrospun onto the collector plate. Detailed spinning and environmental parameters (voltage, flow rate, collector distance, humidity, temperature) needed to achieve optimum continuous spun fibers and to avoid bead formation were listed in Table 1. Electrospun fiber mats were kept on a collector plate for another 12 hours to drive off the residual solvent. The electrospinning was processed in darkness or under yellow light when necessary.

2.2.3 Post-annealing Treatment

Some of the fiber mats were post-annealed upon a pre-heated hot-plate at a desired temperature (detailed information is in Table 2.2). Aluminum plates were placed on the top of the fiber mats during the heating process to avoid shrinkage.

2.2.4 Degradation Test Setup

Degradation testing was performed using a constant wavelength and intensity UV light (254 nm, dose = 2.2 mJ/S*cm^{-2}) as trigger stimulus. Typically, 1 cm × 1 cm samples were cut out of electrospun fiber mats over a glass microscope slide and placed on a hot plate at room temperature (~ 17 °C). Then we adjusted the distance between samples and UV source at 1 cm before beginning

radiation exposure. The entire setup was covered by aluminum foil to avoid light contamination and limit air circulation. To compare degradation properties of various compositions shown in Table 2.1, the samples were exposed for fixed time periods before characterization.

2.2.5 Characterization methods

A Waters ambient temperature gel permeation chromatography (GPC) with THF as solvent was used to measure the molecular weight of polymers against a polystyrene standard. ^{1}H NMR spectra were detected with a Varian INOVA 400 spectrometer at 400 MHz. Thermogravimetric analysis (TGA) was conducted on a TA Instrument Q500 using a heat ramp of 10 °C/min to reach 400 °C. Dynamic mechanical analysis (DMA) for both tensile test and storage modulus were measured on a TA Instrument Q800. The tensile testing with constant force ramp of 1 N/min at room temperature was performed on ASTM D638 Type V specimens. For storage modulus tests, electrospun fiber mats were cut into a rectangular shape (l.w.t) of 2.0 × 1.0 × 0.1 mm, and DMA tests were analyzed at 1 Hz, 0.05 % strain amplitude with a constant static force of 0.1 N. Scanning electron microscopy (SEM) for high resolution micrographs of Pt sputtered samples were captured on a MIRA3-TESCAN through channel SE and the accelerating voltage was 1.0 KV. Transmission electron microscopy (TEM) morphology characterization of RuO_4 stained PPC_{70}/$cPPA_{30}$/$PAG_{5wt\%}$ nanofibers were directly deposited on copper grid and captured on FEI F20 at accelerating voltage of 200 kV.

Scheme 2.1. Concept diagram of electrospun polymer blends fiber mat

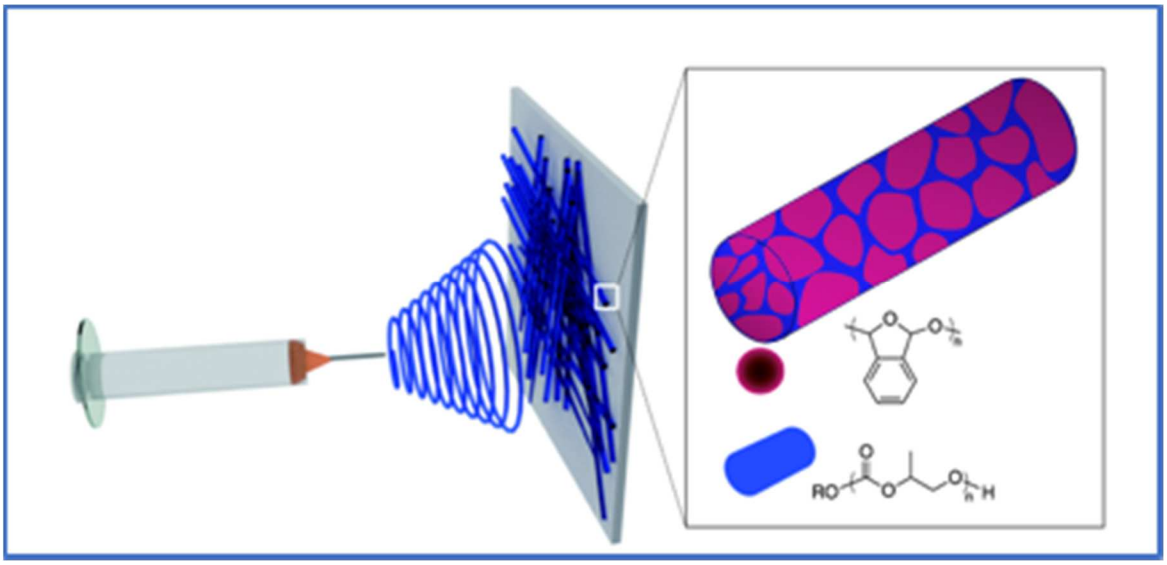

Table 1. Solutions and Electrospinning Conditions

Sample	Solution[a]	Distance (cm)	Voltage (kV)[b]	Flow Rate (mL/h)	T (°C)	Humidity (%)
1	$PPC_{100}/PAG_{5wt\%}$	20	14.40	1	21	60
2	$PPC_{90}/cPPA_{10}/ PAG_{5wt\%}$	20	14.50	1	20	63
3	$PPC_{70}/cPPA_{30}/ PAG_{5wt\%}$	20	14.60	1	21	59
4	$PPC_{60}/cPPA_{40}/ PAG_{5wt\%}$	20	15.50	1	24	53
5	$PPC_{30}/cPPA_{70}/ PAG_{5wt\%}$	20	15.55	1	21	62
6	$PPC_{10}/cPPA_{90}/ PAG_{5wt\%}$	20	15.50	1	22	62
7	$cPPA_{100}/ PAG_{5wt\%}$	20	14.80	1	21	48
8	$PPC_{50}/cPPA_{50}$	20	14.50	1	22	51
9	$PPC_{50}/cPPA_{50}/ PAG_{5wt\%}/AA_{3wt\%}$	20	14.60	1	21	58

[a]The subscripts of PPC/cPPA represent the weight percentage of each polymer in polymer blends. The weight percentage of PAG refers to polymer blends. [b]The electrospinning parameters were modulated by voltage with fixed distance and flow rate according to environmental conditions (temperature and humidity) to produce continuous nanofibers with minimum bead formation as shown in Figure S3 (please refer to Supporting Information).

Table 2. Mechanical properties of $PPC_{50}/cPPA_{50}/PAG_{5wt\%}/AA_{3wt\%}$ fiber mats as a function of post-annealing temperature[a]

Sample	Post-annealing Temperature (°C)	Post-annealing time (min)	Tensile strength (MPa)	Strain (%)	Young's modulus (MPa)[b]	Fiber diameter (nm)
10	21	0	0.696	2.792	43	468.7 ± 102
11	30	30	1.313	1.313	58.46	520.5 ± 198
12	40	30	1.168	1.168	83.72	654.7 ± 213
13	50	30	2.491	4.192	136	666.76 ± 98
14	60	30	2.512	2.520	168.5	809.5 ± 174
15	70	30	2.506	2.956	139.3	film
16	80	30	1.784	4.944	120.2	film

[a]The subscripts of PPC/cPPA represent the weight percentage of each polymer in polymer blends. The weight percentage of PAG/AA refers to polymer blends. [b]Young's modulus was calculated according to the linear part of the stress-strain curve as shown in Figure S7 (please refer to Supporting Information).

2.3 Results and discussions

2.3.1 Electrospun polymer blends

PPC composite fiber mats with good mechanical properties after heat treatment have also possessed good degradation performance under UV light, but additional heat was required to achieve full decomposition. cPPA has shown potential usage in transient microelectronics due to its high acid sensitivity. We blended PPC and cPPA together to investigate any synergistic effects, and based on our prior research, used 5 wt% PAG relative to the polymer blend to initiate acid release by thermal or UV irradiation. Non-woven polymer blend fiber mats were electrospun in various compositions to explore the different characteristics. Electrospinning parameters for multiple compositions of polymer blends were optimized to produce consistent non-woven fiber mats with minimum formation of beads as shown in Figure S3(please see Supporting Information Figure S3 for SEM images of selected electrospun polymer blend fiber mats). To further understand PPC and cPPA heterogeneous morphologies in electrospun nanofibers, RuO_4 stained fiber mats were characterized with TEM as shown by the micrograph in Figure S4 (please see Supporting Information Figure S4 for a detailed illustration). In the micrograph, the darker regions are the stained cPPA which is dispersed in the overall fiber PPC phase indicating a heterogenous mixture of the two phases. Following the nanofiber morphology characterization, Scheme 1 represents the morphology of electrospun PPC/cPPA polymer blend nanofibers, with separate phases representing both cPPA and PPC domains resulting from their immiscibility during electrospinning.

The variations in degradation temperature ($T_{d,\,5wt\%}$) and Young's modulus of the polymer blends with different compositions and fixed PAG content (5 wt% with respect to polymer blend) are shown in Figure 2.1. When the cPPA loading was less than 30 wt%, the degradation temperature

and Young's modulus decreased steadily, since the continuous phase consists of PPC (the addition of cPPA from 0 wt% to 10 wt% caused dramatic decreases in degradation temperature); however, as the amount of cPPA increased, the continuous phase of PPC in the fiber was gradually switched to cPPA, until cPPA exceed 70 wt%, at which point both degradation and mechanical properties of electrospun polymer blends closely resembled that of pure cPPA. The reduction value of both degradation temperature and mechanical strength with respect to increasing amount of cPPA in electrospun solution composition indicates the alternate dominant phase in fiber would determine the fiber mats characteristic behavior.

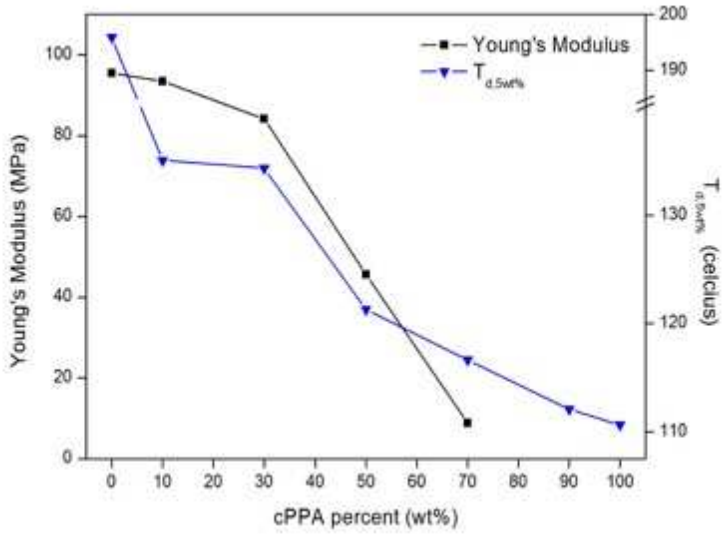

Figure 2.1. Degradation temperature and Young's modulus change trend in relation to different cPPA wt% of electrospun PPC/cPPA polymer blends. All samples showed here contain 5 wt% PAG. The missing Young's modulus data for samples of cPPA over 90 wt% results from the fiber mat being too brittle to cut it on shape for a DMA test.

For completeness we have to mention when the two polymer components are at equivalent weight in the system, it forms a co-continuous phase. Degradation tests of electrospun polymer blends

under UV irradiation at room temperature were investigated. As shown in Figure 2.2, with 5 wt% PAG, UV irradiation released acid which then started chain scission of PPC and cPPA.[47] The full decomposition of electrospun fiber mats were observed with cPPA compositions over 70 wt%, with only a tacky residue left. However, different degrees of shrinkage occurred for fiber mats for cPPA compositions less than 70 wt%.

The UV irradiation test conformed to the analysis presented in Figure 2.1, when cPPA was the continuous phase, the fiber mats exhibited similar properties. Nevertheless, the mechanical properties of UV only degradable samples are extremely poor. Since a minimal amount of solid residue remained after UV irradiation from the polymer blends of PPC/cPPA of 50/50, it was considered the best composition to avoid brittleness in further tests.

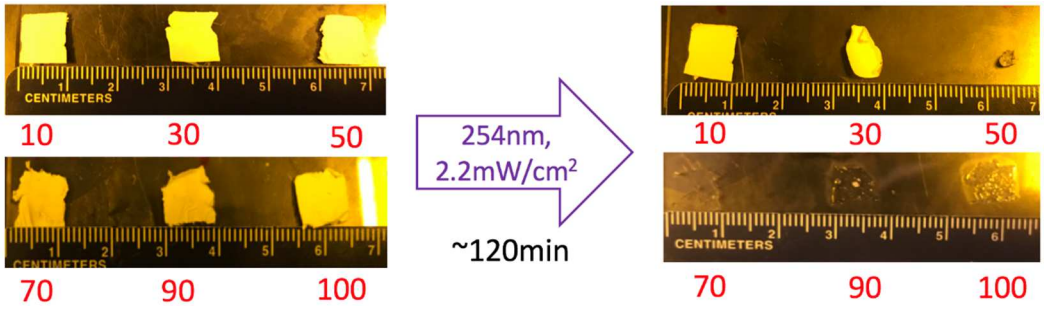

Figure 2.2. Electrospun fiber mat with different cPPA loadings (wt%) (as shown by the red labels) before and after UV (254nm, 2.2mW/cm^2) degradation over ~ 120 min at room temperature. All fiber mats were cut into 1 x 1 cm samples.

Scheme 2. UV-triggered degradation process of PPC_{50}/$cPPA_{50}$/ $PAG_{5wt\%}$/$AA_{3wt\%}$ fiber mat

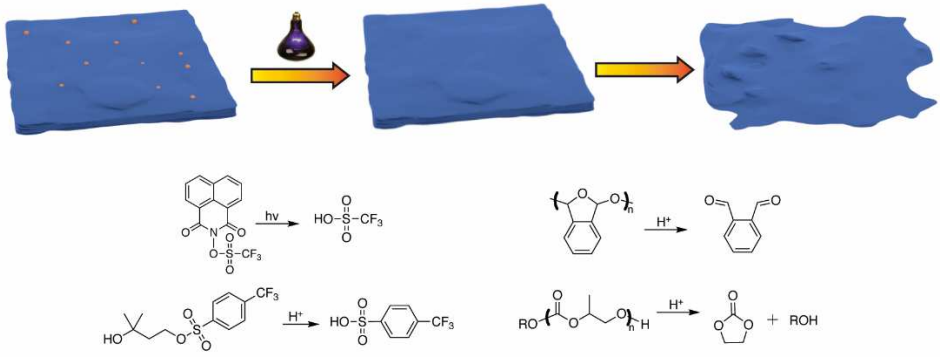

2.3.2 Improving degradation performance

For applications such as a rigid support for transient microelectronic devices, the fiber mat should be stable at room temperature unless triggered by external stimuli. It requires us to improve $PPC_{50}/cPPA_{50}/PAG_{5wt\%}$ fiber mat transient performance without undermining its integrity at room temperature in the absence of triggers. Thus an acid amplifier (AA), was tested.[45] On the basis of electrospun $PPC_{50}/cPPA_{50}/PAG_{5wt\%}$ polymer blend fiber mats, we incorporated 3 wt% of acid amplifier into the system to optimize the degradation performance. The degradation mechanism shown in Scheme 2.2 illustrates the reaction sequence triggered by UV radiation exposure. First, as a result of UV exposure the PAG decomposes to release acid. Subsequently, the AA reacts to produce an additional strong acid and this combination maximizes both the production rate and amount of acid generated in the system. This increased concentration of acid leads to enhanced catalysis of the chain scission of PPC and cPPA, resulting in the fast degradation of the fiber mat.

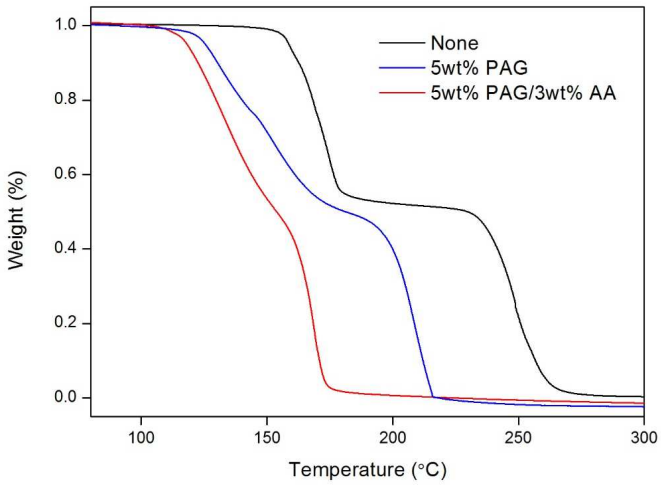

Figure 2.3. TGA trace of electrospun PPC/cPPA polymer blends in fixed composition (50/50) with no acid source (black), PAG (blue) or PAG/AA (red). Samples with both PAG and AA showed superior degradation behavior.

Thermogravimetric analysis (TGA) and gel permeation chromatography (GPC) measurements were done to confirm the degradation as shown in Figures 3 and 4. Comparing polymer blends at

different compositions, the TGA curves in Figure 3 indicate the gradual decrease of T_d with increasing incorporation of PAG and AA. The significant two stage decomposition of $PPC_{50}/cPPA_{50}$ (black curve) is a result of blending of the two kinds of polymers, the first stage being the decomposition of cPPA and the second being the decomposition of PPC. By incorporating 5 wt% PAG into the system (blue curve), the degradation temperature of both polymers decreases dramatically due to their backbones' acid sensitivity. Incorporation of 3 wt% AA results in a decrease in the T_d of PPC to 110 °C, which matches the decomposition temperature of the AA when blended in a phenolic photoresist polymer matrix reported by Kruger. [35]

The depolymerization of $PPC_{50}/cPPA_{50}$ with the addition of PAG and AA was confirmed using GPC by monitoring the molecular weight reduction during UV irradiation. Chromatograms were recorded using both UV and RI detectors, Figures 4a/4c and Figures 4b/4d, respectively. The UV detector was set at a wavelength of 254 nm, so only the cPPA component with aromatic groups in the polymer blend is observed. From the UV signal, a rapid decrease of the peak at 18 min elution time indicates the full decomposition of cPPA after 60 min of UV exposure, which occurs both with and without AA. From the RI, for the fiber mat with only PAG, while there was a rapid decrease in the cPPA peak after 60 min (blue curve), the PPC peak at 17 min elution time decreased slowly and was still prominent after 90 minutes of UV exposure (green curve in 4b). With the addition of 3 wt% AA, there is a significant decrease of the PPC peak at 17 minutes elution time, and the formation of dual peaks at 90 minutes of UV irradiation suggests that the sample was a mixture of species with different molecular weights of PPC.

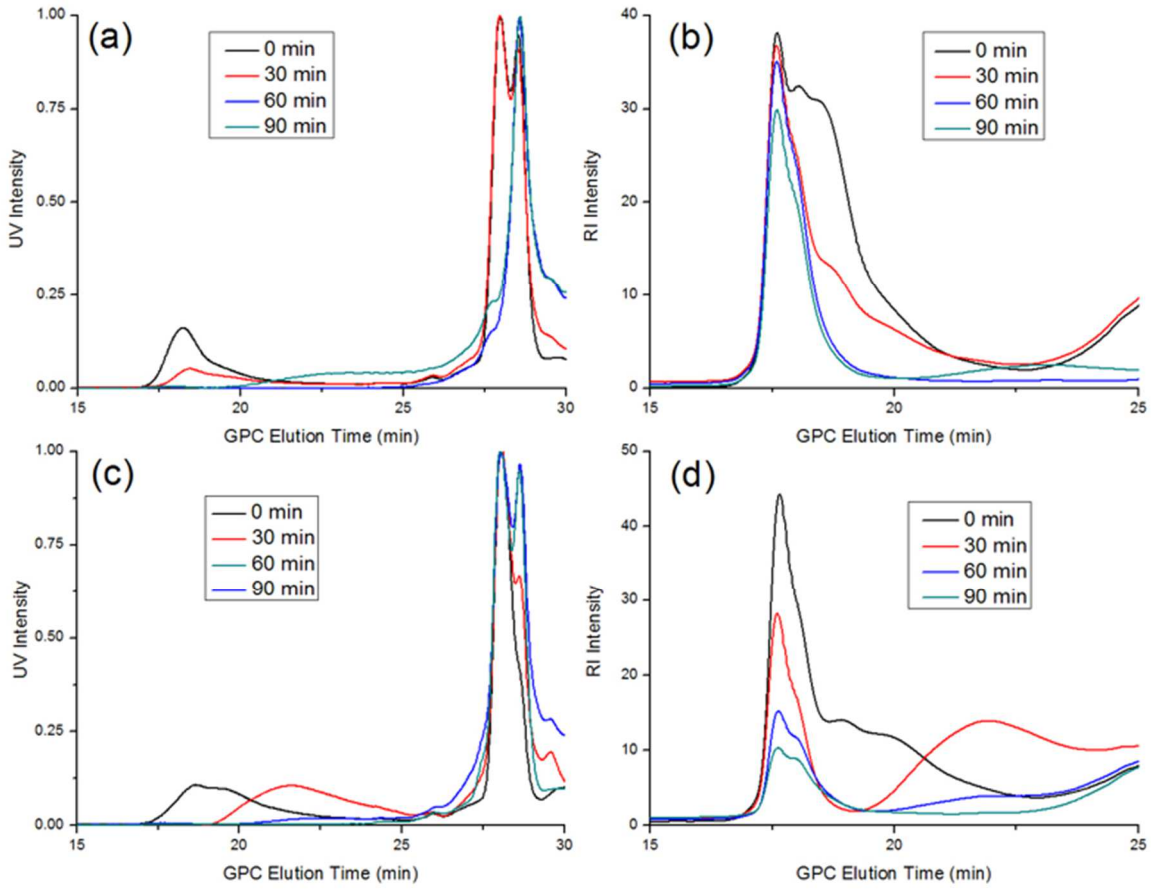

Figure 2.4. Comparison of GPC molecular weight change of electrospun fiber mat in $PPC_{50}/cPPA_{50}$ composition with 5 wt% PAG (4a and 4b) or 5 wt% PAG/3 wt% AA (4c and 4d) under UV irradiation for different exposure period: (a) molecular weight change detected by UV signal of $PPC_{50}/cPPA_{50}/PAG_{5wt\%}$; (b) molecular weight change detected by RI signal of $PPC_{50}/cPPA_{50}/PAG_{5wt\%}$; (c) molecular weight change detected by UV signal of $PPC_{50}/cPPA_{50}/PAG_{5wt\%}/AA_{3wt\%}$; (d) molecular weight change detected by RI signal of $PPC_{50}/cPPA_{50}/PAG_{5wt\%}/AA_{3wt\%}$. The dose of UV light (254 nm, 2.2 mW/cm^2)

Images of the fiber mats before and after UV exposure shown in Figures 5 reveals that the incorporation of 3 wt% AA vastly improves the degradation performance of the $PPC_{50}/cPPA_{50}$/5 wt% PAG at room temperature. There is a negligible amount of residue left visible to the naked eye. SEM characterization, Figure 6, shows that the morphology of the fiber mat was completely destroyed after 90 minutes of UV exposure.

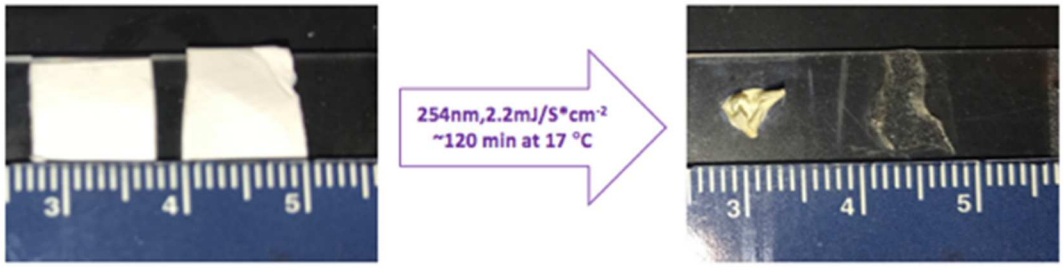

*Left sample: $PPC_{50}/cPPA_{50}/PAG_{5wt\%}$; Right sample: $PPC_{50}/cPPA_{50}/PAG_{5wt\%}/AA_{3wt\%}$

Figure 2.5. UV degradation test of 1 x 1 cm electrospun fiber mats with different compositions, both samples combine both polymers and have PAG, but the right samples also have acid amplifier.

Since mechanical properties are important in our system, the change in storage modulus of the electrospun fiber mat was measured through transient DMA testing while exposing it to UV irradiation (254 nm, dose = 2.2 mW/cm^2) as shown in Figure 7. A dramatic loss of storage modulus up to ~ 85 % was observed with the addition of both the PAG and AA in polymer blends until the failure of fiber mat. The reference specimen with only PAG as an acid source exhibited a much slower decrease under UV irradiation which matches the GPC results above, while the polymer only sample maintained a constant modulus throughout the test. The DMA test emphasizes that the combination of AA and PAG accelerates the degradation process of whole system.

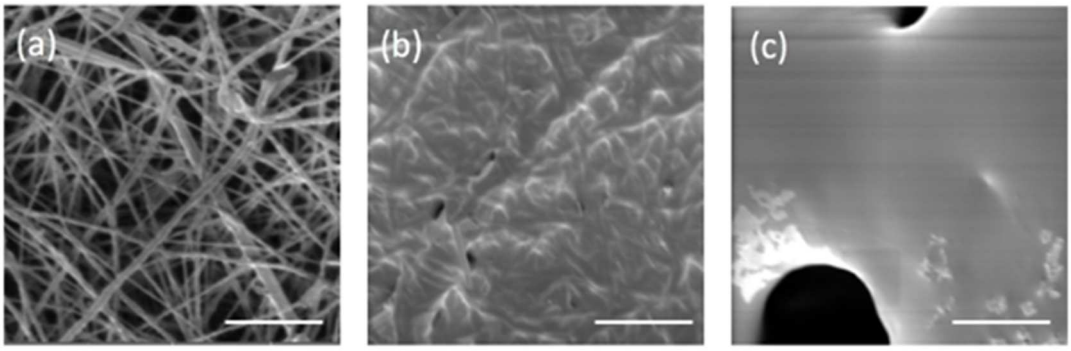

Figure 2.6. SEM characterization of $PPC_{50}/cPPA_{50}/PAG_{5wt\%}/AA_{3wt\%}$ under UV irradiation (254nm, 2.2mJ/S*cm^{-2}) for (a) 0 min; (b) 60 min; (c) 90 min. Scale bar is 5 μm

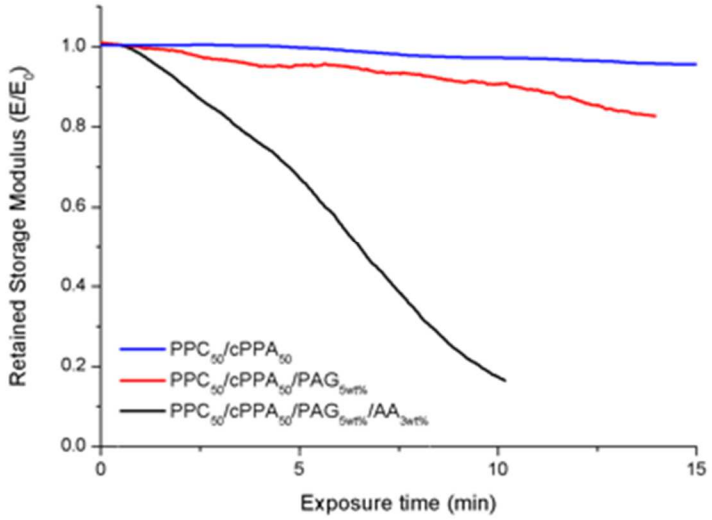

Figure 2.7. Storage modulus trend lines of electrospun fiber mats in different compositions under UV irradiation. All the samples in different composition as shown in the image are cut into fixed rectangular shape and exposed to continuous irradiated until failure.

2.3.3 Strengthening mechanical properties

Consistent with our previous work on electrospun PPC fiber mats, post-annealing effectively enhances mechanical properties by causing the strength of junction points of fibers to increase during heat treatment. M. Kancheva et al. has shown that heat treatment can greatly enhance the mechanical properties of electrospun polymer blend fiber mats. Thus in this investigation, we focused on post-annealing to strengthen the integrity of fiber mats with $PPC_{50}/cPPA_{50}/PAG_{5wt\%}/AA_{3wt\%}$ composition (for detailed condition please see Table 2.2). As shown in Figure 2.8, annealing was performed at a variety of temperatures for a fixed time (30 min). An increase in Young's modulus is observed from 43 MPa to 170 MPa for annealing temperatures up to 60 °C, which is the highest mechanical strength recorded to date for room temperature degradable fiber mats. Higher annealing temperatures resulted in a subsequent decrease in mechanical properties. This reduction can be attributed to the thermally triggered release of acid from the PAG and AA that rapidly degrades the nanofibers. SEM characterization of the post-annealed fiber mats shows similar morphology changes at increasing annealing termperatures as was observed in the UV degradation imaged in Figure 6. This is consistent with our previous work, which showed the formation of films and loss of mechanical properties during post-annealing at higher temperautres.[26] Furthermore, the UV degradation test of the fiber mat annealed at 60 °C was investigated as shown in Figure S9 where full decomposition wasobserved. This result proves that fiber mat degradation is not compromised by post-annealing steps.

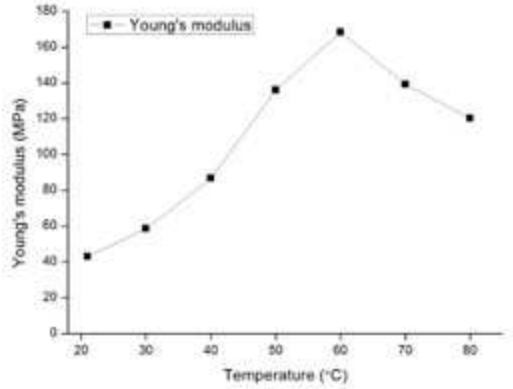

Figure 2.8. Young's modulus of post-annealed fiber mat for fixed time of 30 min. The composition of all samples are $PPC_{50}/cPPA_{50}/PAG_{5wt\%}/AA_{3wt\%}$.

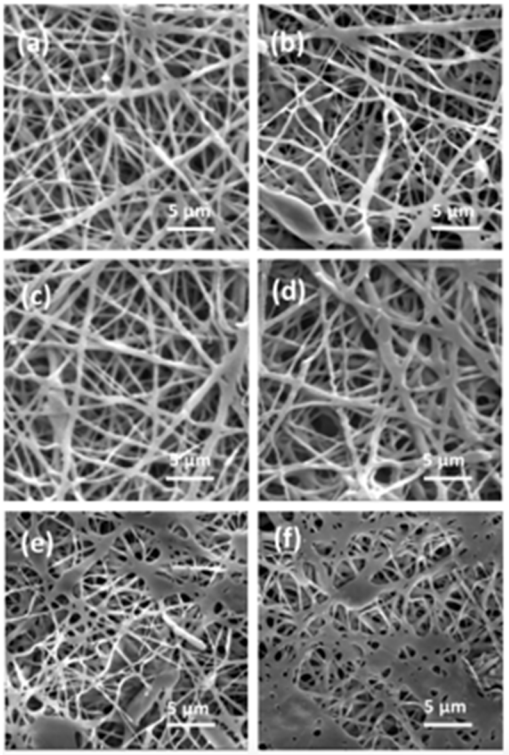

Figure 2.9. SEM images of post-annealed $PPC_{50}/cPPA_{50}/ PAG_{5wt\%}/AA_{3wt\%}$ fiber mat for 30 min at (a) 30 , (b) 40 , (c) 50 , (d) 60 , (e) 70 , (f) 80 °C.

2.4 Conclusion

Considering these results, we have demonstrated a UV-triggered degradable electrospun fiber mat with optimized mechanical properties. In particular, the polymer blends with varied composition have proven that $PPC_{50}/cPPA_{50}$ forms a blend morphology in the fiber mat which enabled the achievement of our desired properties. With the addition of PAG, exposure to UV irradiation released strong acid to decompose the electrospun fiber mat. Besides that, the use of an acid amplifier (AA) is novel to nanofiber spinning and compensates for the limitations of acid generated from PAG through UV exposure. The thermal stability of the AA guarantees the integrity of the fiber mat in the absence of external stimuli, which is essential for many envisaged applications. The acid released from PAG induced by UV irradiation leads spontaneously to further production of acid through the AA, resulting in much more rapid depolymerization and disintegration of the whole system. Since the incorporation of the cPPA component compromises the fiber mat mechanical properties, we employed post-annealing methods to enhance their mechanical properties. The Young's modulus (E) was improved by post-annealing, with 30 min heat treatment at 60 °C to raise E to 170 MPa due to the increased number of junction points. Consequently, the UV responsive degradable polymer fiber mat is applicable to a wide range of solid state applications, such as a transient rigid support for microelectronic devices and packaging materials, in which mild degradable conditions with high mechanical properties would be required.

2.5 Complementary work

While we can proudly announce that so far we have accomplished to produce UV-triggered transient fiber mats with decent mechanical strength for multiple usages, however, complementary research is needed to explore the reason how polymer blend morphology changes in various compositions determine the mechanical and physical properties of the blend.

To observe the two phases distribution in electrospun polymer blends fibers, SEM figures are apparently insufficient since no significant contradistinction between two polymers phases in fibers could be observed as shown in Figure S3 (Supporting Information). Therefore, we have to apply alternative characterization technique to advance our research. According to John S. Trent et al, ruthenium tetraoxide (RuO_4) can selectively enhance electron density contrast for transmission electron microscope (TEM) of heterogeneous polymer systems.[48] In our case, cPPA component in polymer blends contains aromatic moiety which can be stained by RuO_4, meanwhile PPC component would stay intact.

$PPC_{70}/cPPA_{30}$ composition was selected to further our research, first of all, electrospun $PPC_{70}/cPPA_{30}$ fiber mat was stained with RuO_4 overnight. Then fully stained fiber mat was carefully installed in copper grid for further TEM characterization. The results are shown in Figure 2.10, the stained regions are cPPA phase and unstained regions are PPC phase. We can easily conclude from Figure 2.10 that cPPA and PPC polymer blend are immiscible and their blends show heterogeneous morphologies. This result conforms to previous experiment as shown in Figure 2.1, the variation of PPC/cPPA compositions would not linearly change the physical and mechanical properties of polymer blends. Instead, significant conversion of polymer blends properties were observed when cPPA component weight percentage increased continuously. When cPPA component weight percent less than 30, the properties of electropsun polymer blends fiber mats were similar to pure PPC, as cPPA weight percentage increased over 70, the properties of electrospun polymer blends fiber mats were close to pure cPPA. In this two situations, the morphology of one phase dispersed in domains in the other. However, when the weights of cPPA and PPC reached equal in the composition, the electrospun fiber mat exhibited synergistic

properties, which means they have formed co-continuous which gives unique combination of the properties of the components.

Although we can infer from the experimental results that $PPC_{50}/cPPA_{50}$ represents co-continuous morphology of electrospun polymer blends, additional experiments could be done to conform this result in the future. The morphologies of polymer mixing are relied on the relative viscosities and interfacial tension, and we define the co-continuous morphologies when the viscosities of two polymer components are equal in a specific composition. In this case, the coming graduate students who want to continue this project can operate comprehensively viscosities test of two polymer phases in different polymer compositions.

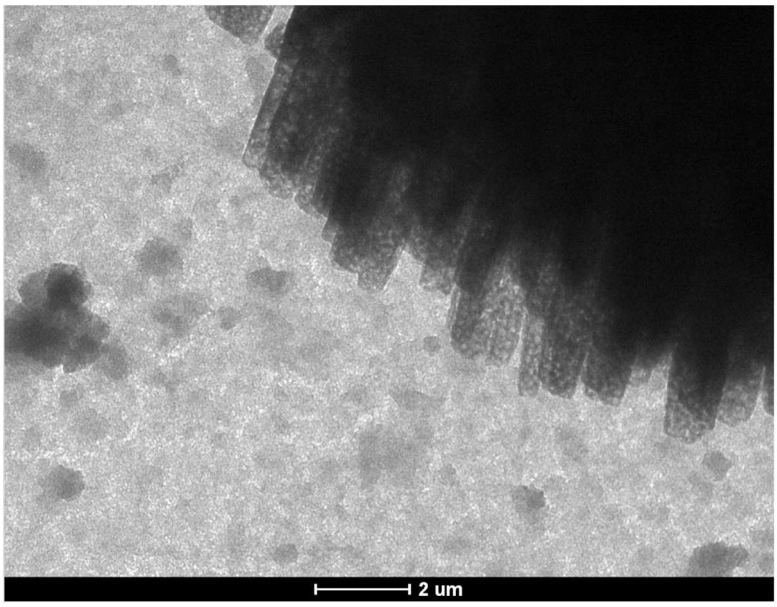

Figure 2.10. TEM characterization of RuO_4 stained electrospun polymer blends nanofibers with $PPC_{70}/cPPA_{30}/PAG_{5wt\%}$ composition in 2 μm scale. The darker domain on a single nanofiber represents cPPA phase.

Chapter 3

3.1 Future goals

In this project, we have managed to realize decomposable PPC/cPPA fiber mats triggered by UV-irradiation at room temperature. The mechanical properties of fiber mats have also been greatly enhanced after post-annealing processing, increasing from ~ 40 MPa to ~ 170 MPa. However, regarding many potential applications such as filters or tissue scaffolds, the mechanical properties of PPC/cPPA fiber mats is still not adequate. Therefore, in this chapter, we will introduce some methods identified from other studies that have proven to effectively reinforce electrospinning fiber mat stiffness apart from post-annealing processing.

3.2 Filler reinforcement

Pure fiber mats normally possess relatively few interactions between fibers in the matrix, so that the weaker interfacial bonding strength and adhesion force inside the fiber mats results in poor mechanical properties, which largely restricts their utilization in day to day use.[49] Therefore, several methods have been developed to compensate for the mechanical limitations of fiber mats, such as incorporating pure fiber mats with coupling agents and surface modification components. In many cases, to achieve substantial mechanical strength improvement, one of the most efficient approaches is by introducing fillers into the fiber matrix.

Fillers and electrospinning in combination are commonly used to produce composite nanofibers, whose properties can be significantly improved with respect to the matrix alone by using different fillers mixed into the fiber matrix.[50] Therefore, it's necessary to explore the possible combinations of fillers and depolymerizable polymers to harness synergistic effects that are capable of expanding the working properties of composite nanofibers. Thus a proper selection of filler and polymer

matrix composition may aid in developing composite nanofiber materials for applications in multiple fields such as the aerospace and automotive industries.[51]

The nanoscale fillers widely used in electrospinning of fiber mats include nanoclays, carbon nanotubes and nanometals. One facet to diminished mechanical properties of fiber matrix (weaker than bulk properties) is polymer viscosity. Electrospinning fiber mats from solutions with large viscosity and lower conductivity tend to produce beads on fiber mats, which are known to compromise the mechanical performances. In this case, the introduction of nano-scale fillers into the system can result in a wide distribution range on fiber mats. Therefore, the wide range distribution of fillers would reduce the polymers solutions viscosity, so the flow of the fibers increases can subsequently reduce their possibility of beads formation. In addition, to enhance the mechanical strength of fiber mats, some studies have shown that those nanoscale fillers have the ability to increase thermal stability of low cost fiber mats compared to expensive high-performance materials.

Therefore, we are expecting to achieve mechanical enhancement by incorporating appropriate nanofillers to our original PPC/cPPA polymer blend fiber mats, for instance, carbon nanotube and nano-clay are introduced as two potential candidates in this paper.

3.2.1 Carbon nanotube reinforcement

Carbon nanotubes have attracted great interest in recent decades due to their remarkable properties. A carbon nanotube can be described as a hollow cylindrical structure with 1 – 2 nm diameter as shown in Figure 3.1 below.[52] According to the cylindrical structure of carbon nanotubes, it can be defined in two forms as single-walled carbon nanotubes (SWCNT) and multi-walled carbon nanotubes (MWCNT).

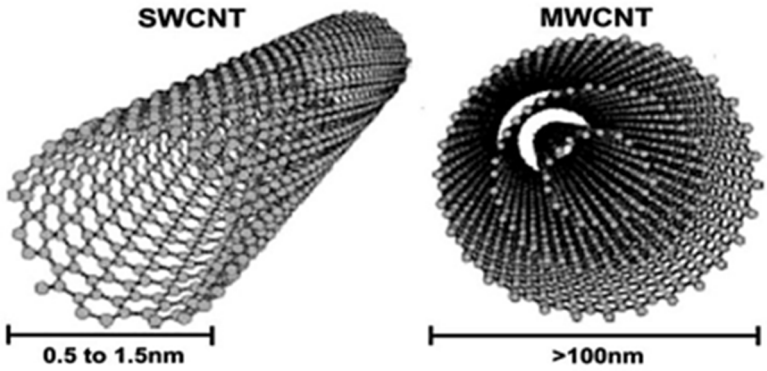

Figure 3.1. Structure of single-walled carbon nanotubes (SWCNT) and multi-walled carbon nanotubes (MWCNT). [53]

Because of its covalent bonding, carbon nanotubes are similar to graphite which arises from their sp^2 hybridization, thus carbon nanotubes possess physical properties similar to graphite such as conductivity and thermal conductivity. Furthermore, with respect to mechanical properties, carbon nanotube also exhibits high tensile strength (~ 100 - 500 GPa), elastic modulus (~ 1 – 5 TPa) and extremely high flexibility due to their porous nanotube structure. Therefore, carbon nanotubes have been explored in the field of polymeric fiber mats for production of polymer-carbon nanotube composites with enhanced properties. According to reports in the literature, the carbon nanotube mixed polymer fiber matrix can potentially provide significant enhancement to both fiber mat modulus and strength since the interfacial shear strength in a carbon nanotube and fiber matrix

composite is much larger than pure fiber matrix alone. In addition, carbon nanotubes are capable of increasing the melting-temperature, glass-transition temperature and thermal decomposition temperature of a polymer matrix.

Here we will present representative research from Robert C. Haddon and his co-workers on electrospun single-walled carbon nanotube (SWCNT) reinforced polystyrene and polyurethane nanofibers.[53] The ester functionalized form of SWCNTs cannot easily be dispersed in the organic solvent without agglomeration which is known to significantly affect the mechanical properties of fiber mats. Furthermore, the incorporation of the esters can improve chemical compatibility of SWCNTs with polymers and exfoliate the SWCNTs bundles as well. The stress-strain measurements of both electrospun ester functionalized SWCNTs reinforced polyurethane (EST-SWNT-PU) fiber mats and SWCNTs reinforced polyurethane (AP-SWNT-PU) are shown in Figure 3.2 below, the significant increase of mechanical properties with respect to SWCNTs and ester-functionalized SWCNTs additives confirming the general features of the above theory.

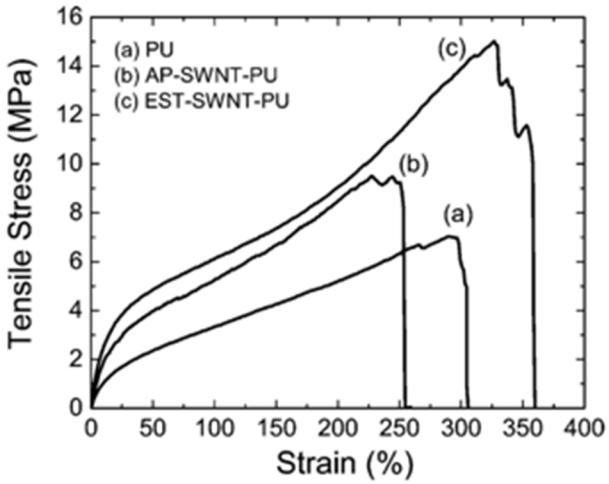

Figure 3.2. Stress-strain curve for electrospun fiber mat composed of polyurethane (PU), SWNT-reinforced polyurethane (AP-SWNT-PU) and ester functionalized SWNT polyurethane (EST-SWNT-PU).[54]

3.2.2 Nano-clay reinforcement

Nanoclay, known as organo-modified montmorillonite (OMMT), is commonly used as a reinforcement component in polymeric fiber matrix. The various polymer/OMMT systems have been extensively investigated since OMMT can contribute to a fibers' improvement in mechanical properties such as thermal resistance and mechanical strength.[54] In recent decades, accompanied by the development of electrospinning, different types of polymer/OMMT nanocomposites have been produced with enhanced mechanical properties, including polyamide 6/OMMT, polystyrene/OMMT and poly(propylene carbonate) (PPC)/OMMT. Herein, we will also introduce our prior research to convey the potential use of OMMT for our electrospun PPC/cPPA polymer blend fiber mats.[24]

The goal of this prior research was to fabricate transient PPC fiber mats with superior mechanical properties. OMMT (20 Å) was incorporated into the system to enhance the mechanical properties of the PPC fiber mat. First, to avoid a significant increase of thermal decomposition temperature, the amount of OMMT introduced to the PPC fiber matrix was limited to a minimum quantity. Consequently, the preparation of PPC/OMMT in DMA solution required ultra-sonication to minimize agglomeration effects of the OMMT which is known to compromise the mechanical properties of a fiber mat. Finally, electrospinning parameters and post-annealing conditions were optimized to reach our desired properties.

The amount of OMMT added to a PPC/PBG system was investigated as shown in Table 1, for clarification, a photo-base-generator (PBG) was added as a stimuli-response photochemical trigger to release base. Though with 5 % PBG incorporated, the PPC fiber mat exhibited its lowest decomposition temperature and highest mechanical properties, the fiber mat was shrank up to ~ 20 % during storage. We can observe from Table 3.1 that adding 5 % OMMT would slightly

change the decomposition temperature of the PPC/PBG fiber mat from 146.2 °C to 154.9 °C; however, when the amount of OMMT reached 10% with respect to PPC, the decomposition temperature increased significantly to 169.4 °C. The combination of OMMT and PBG would reduce the Young's modulus of the fiber mat from ~77.7 MPa to ~54.5 MPa because the interaction between PBG and OMMT would compromise the interfacial reaction between OMMT and PPC fibers.

Table 3.1. Tensile strength and Young's modulus of PPC/OMMT/PBG fiber mat

Amount of additives respect to PPC (weight percent)	Decomposition temperature (°C)	Fiber diameter (nm)	Tensile strength (MPa)	Young's modulus (MPa)
5% PBG	146.2	244 ± 110	4.1 ± 0.2	123.9 ± 4.3
5% OMMT	228.2	261 ± 133	2.8 ± 0.1	77.7 ± 1.5
5% OMMT, 5% PBG	154.9	248 ± 108	2.2 ± 0.9	54.5 ± 12.0
10% OMMT, 5% PBG	169.4	146 ± 60	3.0 ± 0.6	105 ± 26.9

Next, various annealing treatments were applied to PPC/$OMMT_{5\%}$/$PBG_{5\%}$ fiber mats as shown in Figure 3.3a, illustrating that post-annealing at 40 °C exhibited the highest Young's modulus and tensile strength. Then, the post-annealing process at 50 °C at different times was investigated for PPC/OMMT/PBG represented in Figure 3.3b showing the highest Young's modulus and tensile strength. The dramatic mechanical enhancement of PPC/$OMMT_{5\%}$/$PBG_{5\%}$ resulted from either fiber mat densification or fiber mat internal bonding. Since shrinkage was purposely avoided during post-annealing process, it's likely that OMMT caused enhanced overlapping junction point in fiber mats. But when post-annealing time at 50 °C exceeded 40 min, the mechanical properties of the fiber mat decreased due to the decrease of degree of order of the polymer chains among fiber mats induced by electrospinning and exfoliation of OMMT with its agglomeration. Based on

annealing tests of PPC/OMMT/PBG fiber mats, the mechanical properties could be modulated from 54.5 MPa to 746.8 MPa. This remarkable mechanical strength enhancement could allow this transient composite fiber mats to be useful for a wide range of applications.

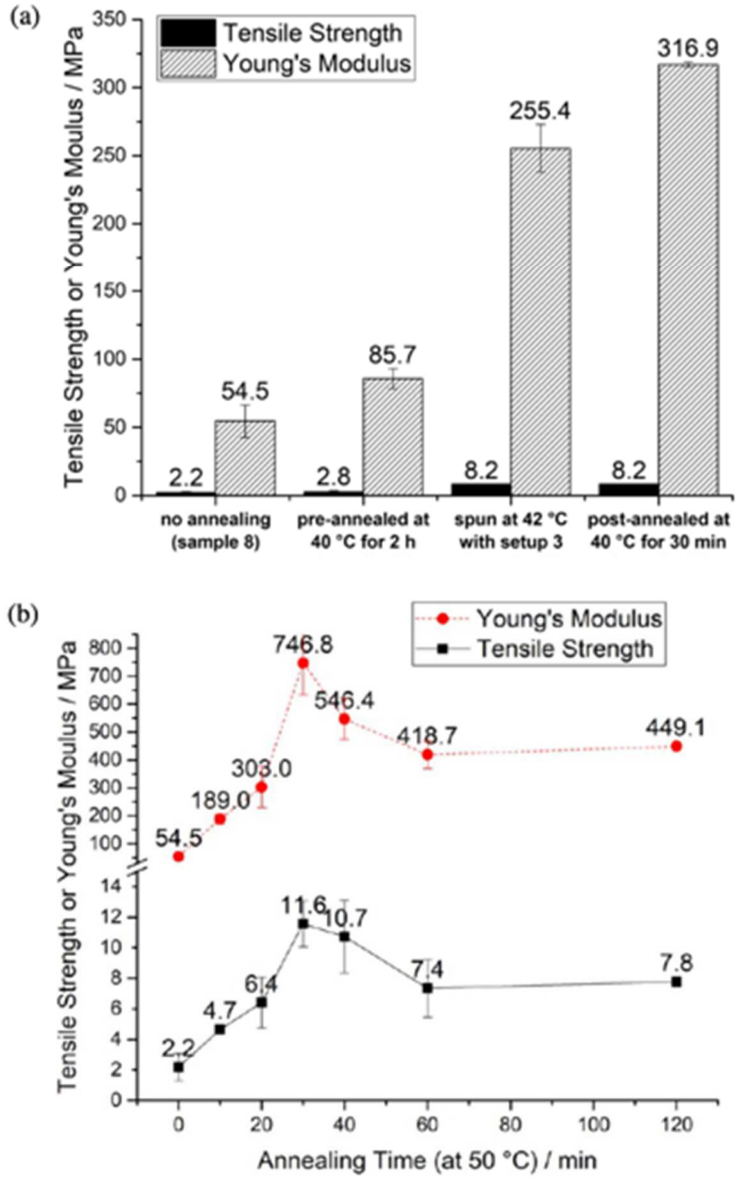

Figure 3.3. Tensile strength and Young's modulus variation of PPC/OMMT/PBG fiber mats in (a) different annealing process type (b) different annealing time at fixed temperature. [24]

3.3 Advanced electrospinning set-up

Our electrospinning conditions to produce PPC/cPPA fiber mats is a typical horizontal set-up including metallic capillary connected to high voltage and a collector with negative charge as shown in Figure 3.4.[53] This traditional set-up can successfully fabricate continuous nanofiber from PPC/cPPA polymer blend solutions as discussed in Chapter 2. However, due to the instability of jet ejected from capillary, the fibers collected are normally randomly oriented structure, which would impair the mechanical strength of fiber mat. Therefore, according to literature, highly aligned fiber structure produced by modified electrospinning set-up as shown in Figure 3.5 is very important to help optimize mechanical strength of fiber mat.[55] In this case, despite adding nano-fillers to original composition, increasing alignment of fiber structure can be used to enhance the mechanical properties of PPC/cPPA fiber mat. Here we will introduce an advanced electrospinning set-up to fabricate orientated fiber mat.

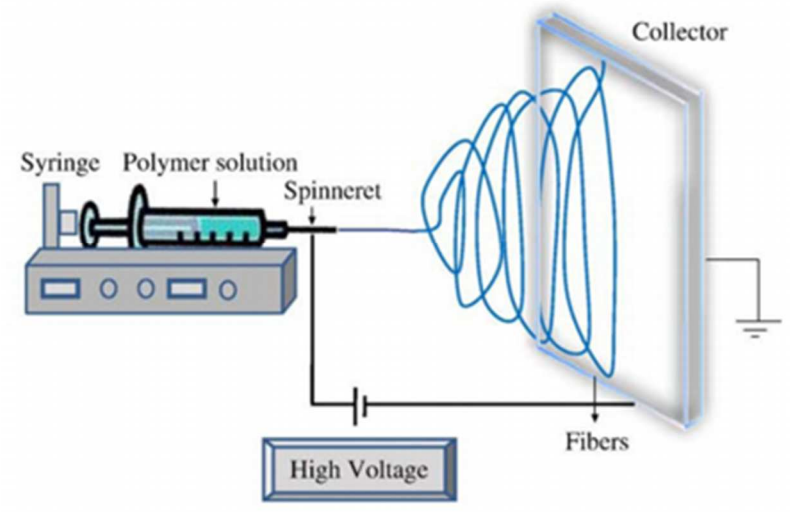

Figure 3.4. Traditional Horizontal electrospinning set-up. [53]

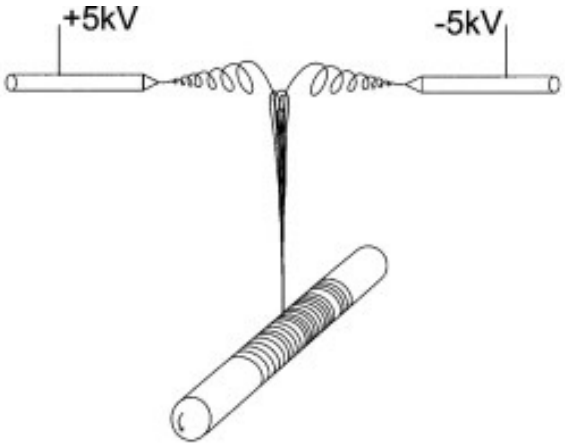

Figure 3.5. Modified electrospinning set-up to fabricate orientated nanofiber structure. [55]

3.3.1 Aligned polymer fiber electrospinning set-up

In this section we will refer work done by Chaobo Huang et al,[56] who managed to significantly enhance the mechanical strength of polymer nanofiber mats through combing methods of adding multi-walled nano-carbon tube (MWNCT) and modified electrospinning set-up to fabricate orientated fiber structure. The SEM characterizations of non-aligned and aligned nanofiber structure are shown in Figure 3.6. Mechanical testing results are shown in Table 3.2 to indicate the tensile strength of polymer fiber mats depend on both the alignment of nanofiber structure and the incorporating of MWNCTs additives. To be clarify, the prepared electrospun polymer solution with MWNCTs are cured at high temperature to enhance the interfacial interaction between MWNCTs and nanofibers. According to Table 3.2, the non-aligned fiber mats tensile strength can be increased from 40MPa to 187MPa by increasing the nanofibers alignment to ~80%. Then by incorporating MWNCTs fillers with high temperature curing, the tensile strength would be significantly increase to 663.7MPa.

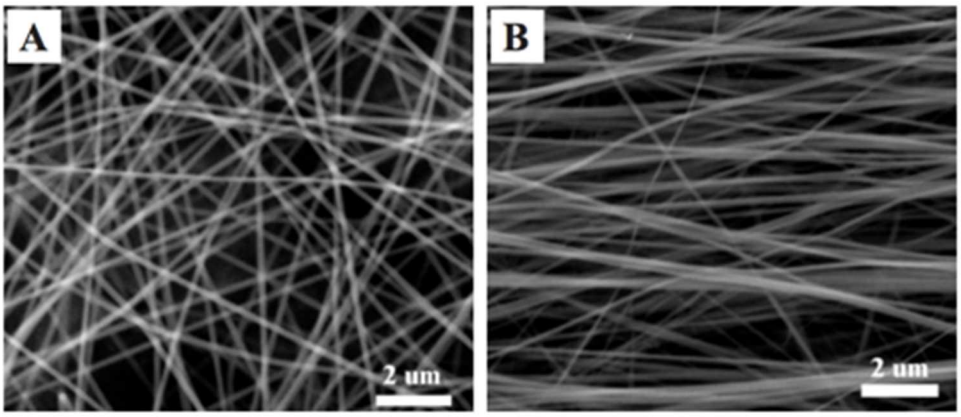

Figure 3.6. Electrospun polymer fiber mats. (A) Non-aligned and (B) aligned with rotating collector. [56]

Table 3.2. Tensile strength of electrospun polymer nanofiber mats [56]

Electrospinning composition	Pure polymer	Polymer with MWCNTs	Polymer with MWCNTs
Curing temperature (°C)/time (min)	100/120	100/120	430/30
Alignment	Non-aligned	~80% Aligned	~80% Aligned
Strain(%)	9.24	10.3	4.97
Tensile Strength(MPa)	40	187	663.7

3.4 Alternative low-ceiling temperature polymer

In the previous sections we have discussed some developed methods to enhance mechanical strength of electrospun polymer fiber mats, then in this section we will introduce an alternative low-ceiling temperature polymer with potentially usage for transient fiber mat. Referring to our previous research about transient electrospun PPC fiber mat,[24] the depolymerization process of PPC was proved to be more sensitive in response to photo-base-generator (PBG) compared to photo-acid-generator (PAG). Regarding this circumstance, we will refer a photo induced depolymerizable poly(olefin sulfone)s with photo-base generating groups in the side chain from

Hirosaki Yaguchi et al's work,[10] and replacing cPPA component in the polymer blends with it since cPPA phase induce the brittleness in the polymer blend fiber mat.

Poly(olefin sulfone)s have gained attention in recent years because of their versatile functionalized side chain which can initiate depolymerization in responsive to heat, high energy irradiation or base. According to Hirosaki Yaguchi et al's work,[10] the depolymerization of poly(olefin sulfone)s is triggered by photo-responsive side group and followed by releasing of protected base in side group to attack the backbone of poly(olefin sulfone) as shown in Figure 3.7. Therefore, fully depolymerization process of poly(olefin sulfone)s by low-energy irradiation can be accomplished, which is favored as transience devices since minimize energy cost is important. Besides that, Olivia P. Lee et al have accomplished to manipulate thermally decomposition temperature of poly(olefin sulfone)s from ~213ºC to ~90ºC through changing the *tert*-butyl carbonate group in the side chain as shown in Figure 3.8.[9] By manipulating side-chain substitutions, they are capable to increase side chain thermal stability to increase decomposition temperature since the thermal decomposition process of poly(vinly butyl olefin sulfone)s is carbonate elimination as rate-

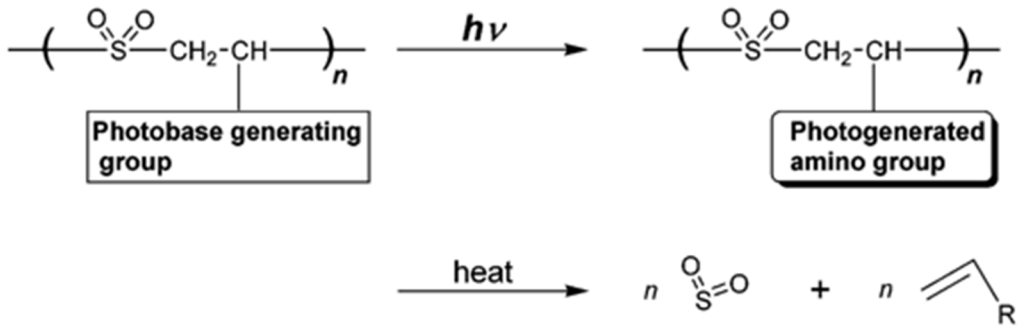

Figure 3.7. Photo-triggered depolymerization mechanism of poly(olefin sulfone)s with photo-base-generator group in the side chain. [10]

determination step. Therefore, with decreasing side-chain branching at β-carbon as shown in Figure 3.8, the decomposition temperature of polymers increase as well.

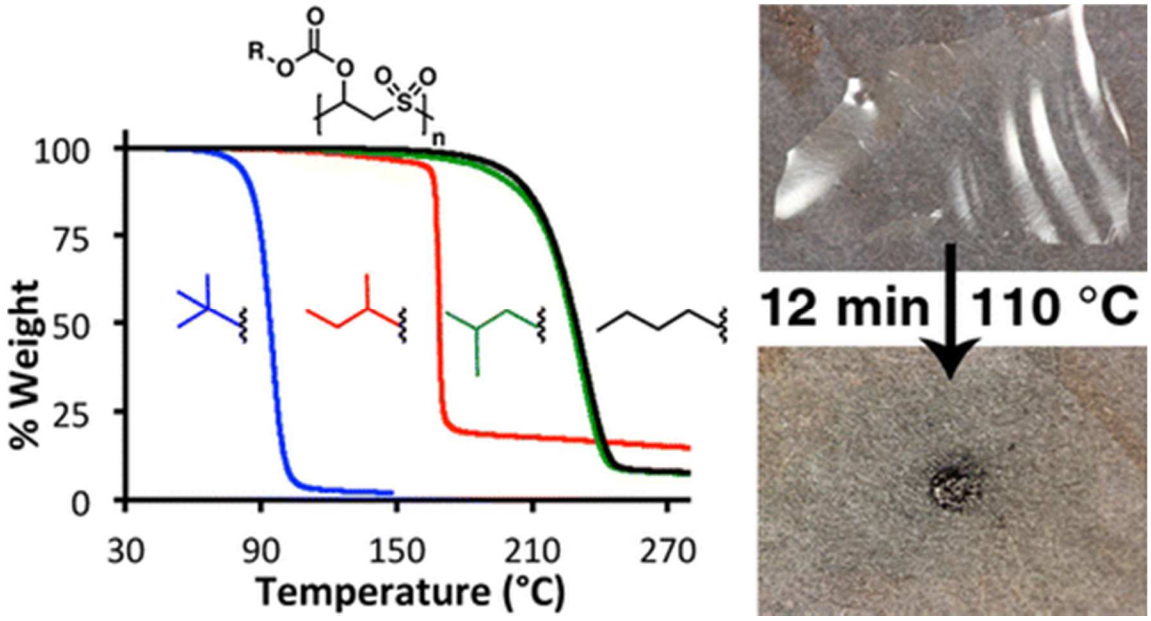

Figure 3.8. Thermal gravimetric analysis (TGA) comparison of poly(vinly butyl olefin sulfone)s with various *tert*-butyl carbonate structure in the side chain. [9]

3.5 Conclusion

Based on the extensively developed studies of polymer/nano-particles composites fiber matrix, we think a filler would be a plausible method to increase the mechanical property of electrospun PPC/cPPA composite fiber mat. Our previous research has proven the positive mechanical reinforcement of OMMT (20 Å) in a PPC fiber mat. However, little investigation has been done to incorporate small amounts of 20 Å OMMT into PPC/cPPA/PAG/AA system and mechanical reinforcement effect. The reason for this could be the interfacial interaction between 20 Å OMMT and PPC phase in the fiber is inhibited by cPPA phase and PAG/AA components; therefore, reducing the size of OMMT from 20 Å to 10 Å could be helpful to increase the interaction effect.

In addition, single walled carbon nanotubes (SWCNT) could be an alternate filler to enhance the mechanical strength of PPC/cPPA polymer blend fiber mats due to its distinguished performance in a variety of polymer/SWCNT nanocomposites. Also by replacing our horizontal electrospinning set-up to modified electrospinning set-up with rotator collector to produce highly oriented nanofiber have been proved to largely enhance the mechanical strength of polymer fiber mats. So I believe the combination of nano-fillers and modified electrospinning set-up can optimize the mechanical property of transient electrospun PPC/cPPA polymer blend fiber mat. Besides, poly(olefin sulfone)s have been introduced as potential candidates to fabricate transient electronic devices due to its versatile functionalized stimuli-responsive group in the side chain. For instance, the protected base in the side chain of poly(olefin sulfone)s could be released by exposing to low energy irradiation and initiate depolymerization of backbone, which is intriguing since base sensitivity of PPC backbone have been proved in our previous research. Thus the transient electronic device made of PPC/Poly(Olefin Sulfone) polymer blend could be achieved with minimum energy required.

Supporting Information

Contents:

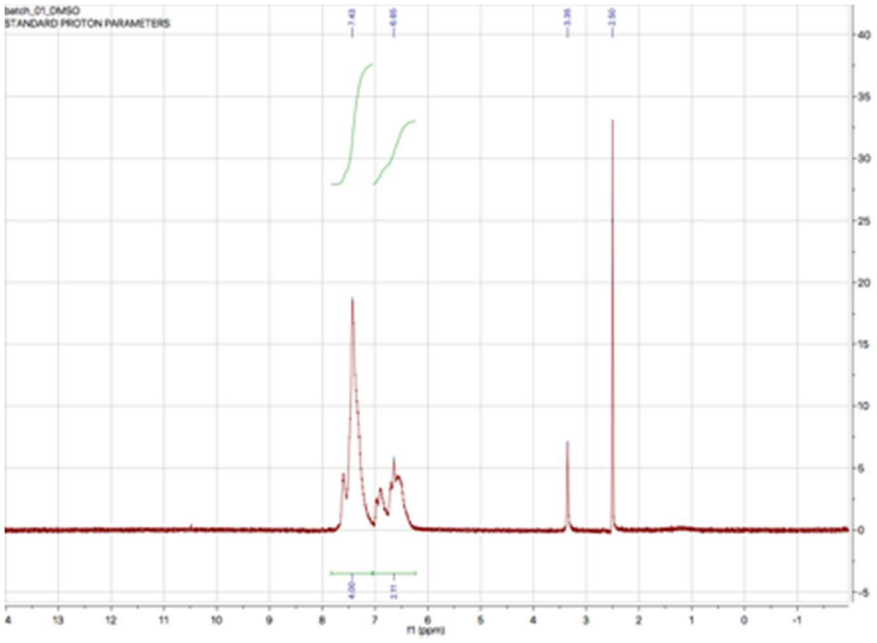

Figure S1. NMR spectra of cyclic-polyphthalaldehyde (cPPA)

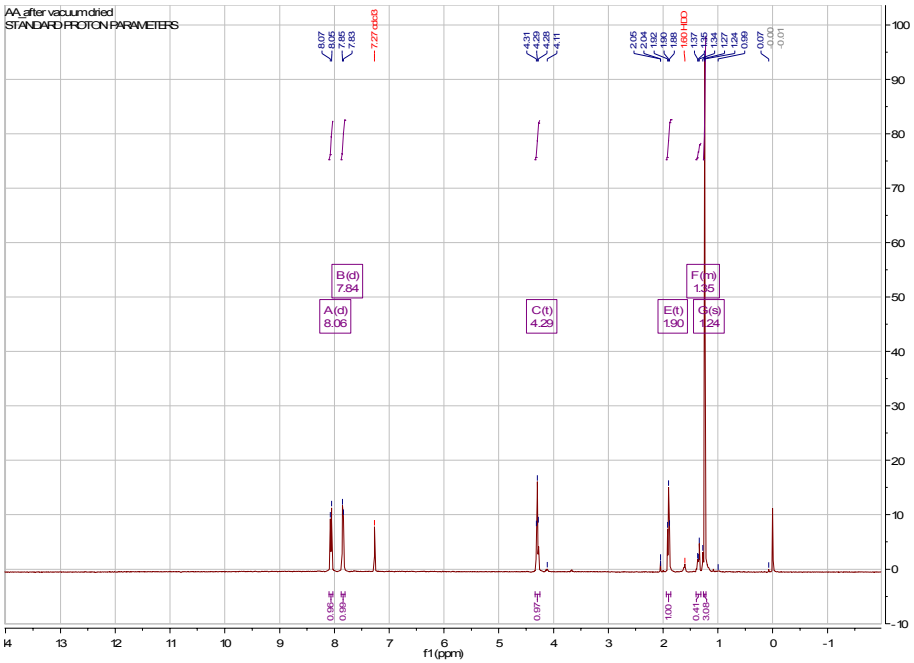

Figure S2. NMR spectra of 3-hydroxy-3-methylbutyl 4-(trifluoromethyl) benzenesulfonate (Acid Amplifier).

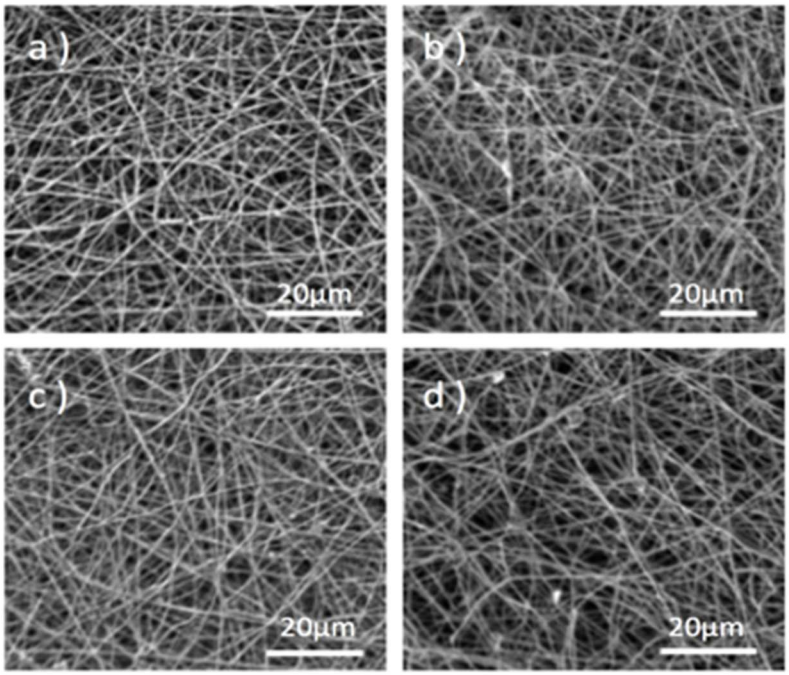

Figure S3. SEM images of selected fiber mats: (a) $PPC_{30}/cPPA_{70}/ PAG_{5wt\%}$ (sample 5), (b) $PPC_{50}/cPPA_{50}/ PAG_{5wt\%}$ (sample 4); (c) $PPC_{70}/cPPA_{30}/ PAG_{5wt\%}$(sample 3), (d) $PPC_{90}/cPPA_{10}/ PAG_{5wt\%}$ (sample 2).

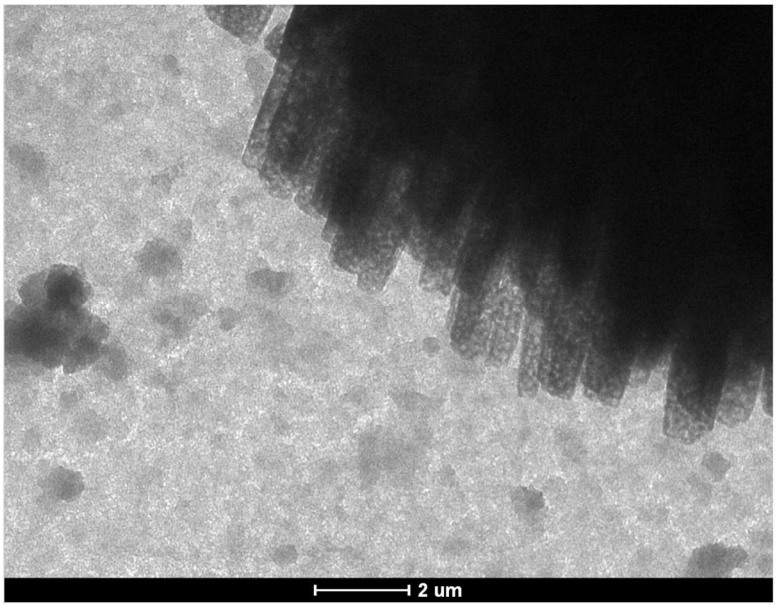

Figure S4. TEM characterization of RuO_4 electrospun $PPC_{70}/cPPA_{30}$ polymer blend fiber mats.

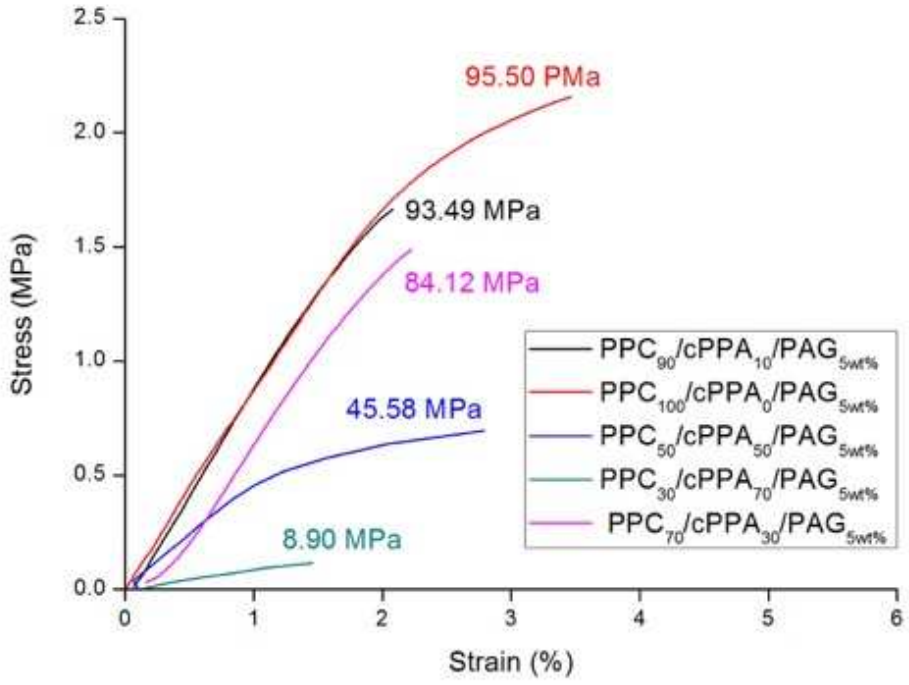

Figure S5. Stress-strain curves of fiber mats in different compositions. Young's modulus

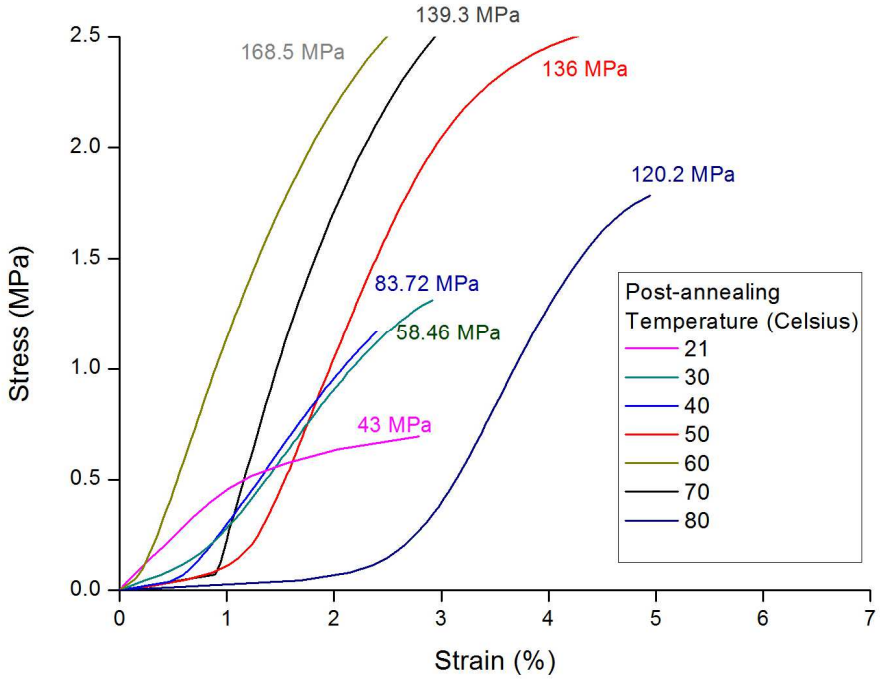

Figure S7. Stress-strain curves of $PPC_{50}/cPPA_{50}/PAG_{5wt\%}/AA_{3wt\%}$ fiber mats after post-annealing process. Young's modulus (E) is labeled with the same color.

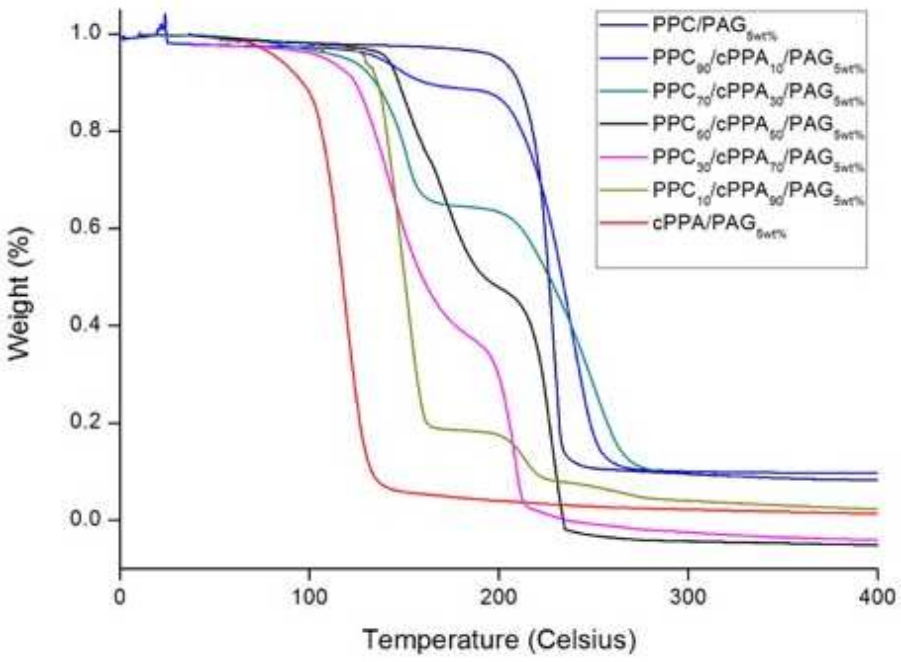

Figure S6. TGA curves of fiber mats in different compositions.

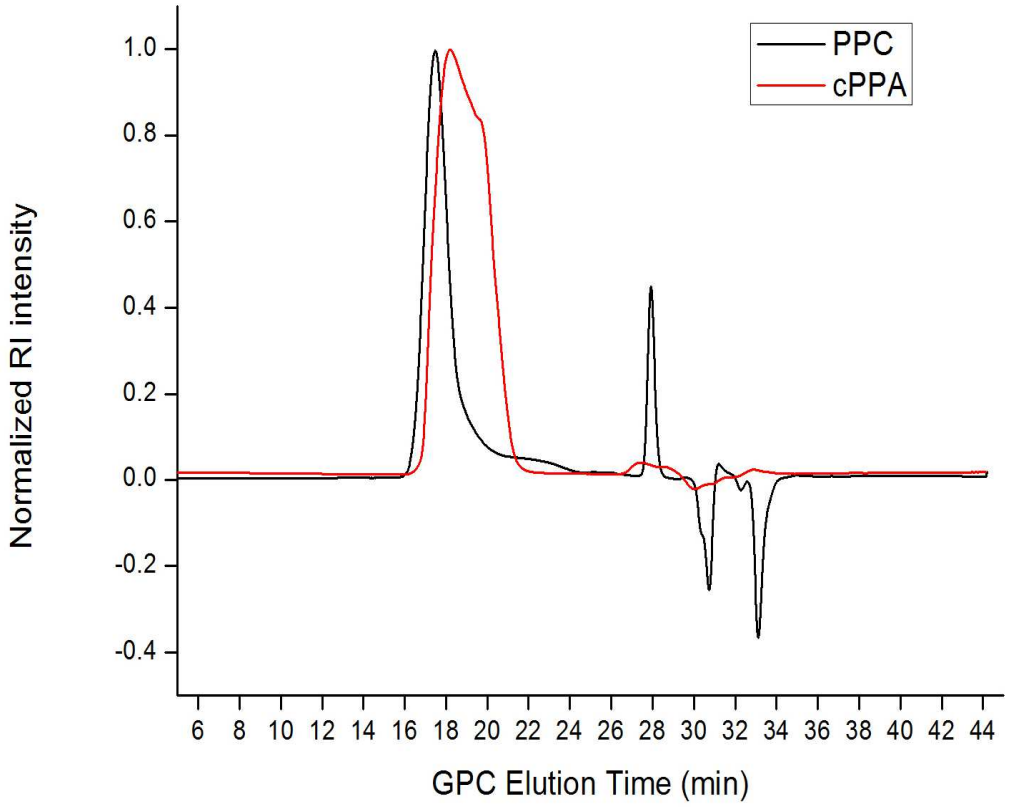

Figure S8. GPC spectra of pure PPC and cPPA polymers.

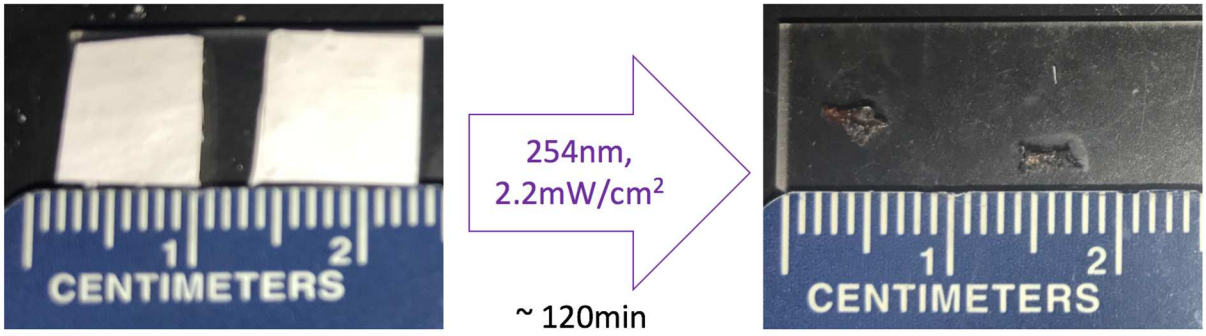

Figure S9. UV degradation test of electrospun $PPC_{50}/cPPA_{50}/PAG_{5wt\%}/AA_{3wt\%}$ fiber mats. The sample in the left was post-annealed at 60 °C for 30 min and the right sample was non-annealed. Both samples exhibited full decomposition under UV exposure at room temperature for ~ 120 min.

Reference

(1) Peterson, G. I.; Larsen, M. B.; Boydston, A. J. Controlled Depolymerization: Stimuli-Responsive Self-Immolative Polymers. *Macromolecules* **2012**, *45* (18), 7317–7328.

(2) Stuart, M. A. C.; Huck, W. T. S.; Genzer, J.; Müller, M.; Ober, C.; Stamm, M.; Sukhorukov, G. B.; Szleifer, I.; Tsukruk, V. V.; Urban, M.; et al. Emerging Applications of Stimuli-Responsive Polymer Materials. *Nature Materials*. Nature Publishing Group 2010, pp 101–113.

(3) Kaitz, J. A.; Lee, O. P.; Moore, J. S. Depolymerizable Polymers: Preparation, Applications, and Future Outlook. *MRS Commun.* **2015**, *5* (02), 191–204.

(4) Patrick, J. F.; Robb, M. J.; Sottos, N. R.; Moore, J. S.; White, S. R. Polymers with Autonomous Life-Cycle Control. *Nature* **2016**, *540* (7633), 363–370.

(5) Dainton, F. S.; Ivin, K. J. Some Thermodynamic and Kinetic Aspects of Addition Polymerization. *Q.Rev.Chem.Soc.London* **1958**, *12(1)*, 61–91.

(6) Phillips, S. T.; Robbins, J. S.; Dilauro, A. M.; Olah, M. G. Amplified Responses in Materials Using Linear Polymers That Depolymerize from End-to-End When Exposed to Specific Stimuli. *J. Appl. Polym. Sci.* **2014**, *131* (19), 1–12.

(7) Sagi, Amit, et al. "Self-immolative polymers." *Journal of the American Chemical Society* 130.16 (2008): 5434-5435.

(8) Li, J.; Nagamani, C.; Moore, J. S. Polymer Mechanochemistry: From Destructive to Productive. *Acc. Chem. Res.* **2015**, *48* (8), 2181–2190.

(9) Lee, O. P.; Lopez Hernandez, H.; Moore, J. S. Tunable Thermal Degradation of Poly(Vinyl Butyl Carbonate Sulfone)s via Side-Chain Branching. *ACS Macro Lett.* **2015**, *4* (7), 665–668.

(10) Yaguchi, H.; Sasaki, T. Photoinduced Depolymerization of Poly (Olefin Sulfone) s Possessing Photobase Generating Groups in the Side Chain. **2007**, *40(26)*, 9332–9338.

(11) Jiang, Y.; Fréchet, J. M. J. Design and Synthesis of Thermally Labile Polymers for Microelectronics. Poly(Vinyl Tert-Butyl Carbonate-Sulfone). *Macromolecules* **1991**, *24* (12), 3528–3532.

(12) Uzunlar, E.; Schwartz, J.; Phillips, O.; Kohl, P. A. Decomposable and Template Polymers: Fundamentals and Applications. *J. Electron. Packag.* **2016**, *138* (2), 020802.

(13) Lv, A.; Cui, Y.; Du, F. S.; Li, Z. C. Thermally Degradable Polyesters with Tunable Degradation Temperatures via Postpolymerization Modification and Intramolecular Cyclization. *Macromolecules* **2016**, *49* (22), 8449–8458.

(14) Esser-Kahn, A. P.; Odom, S. A.; Sottos, N. R.; White, S. R.; Moore, J. S. Triggered Release from Polymer Capsules. *Macromolecules* **2011**, *44* (14), 5539–5553.

(15) Fan, B.; Gillies, E. R. Poly(Ethyl Glyoxylate)-Poly(Ethylene Oxide) Nanoparticles: Stimuli- Responsive Drug Release via End-to-End Polyglyoxylate Depolymerization. **2017**.14(8), 2548-2559.

(16) Schwartz, J.; Kohl, P. A. Decomposable and Template Polymers : Fundamentals and Applications. **2017**, *138* (2), 1–15.

(17) Gergely, R. C. R.; Pety, S. J.; Krull, B. P.; Patrick, J. F.; Doan, T. Q.; Coppola, A. M.; Thakre, P. R.; Sottos, N. R.; Moore, J. S.; White, S. R. Multidimensional Vascularized Polymers Using Degradable Sacrificial Templates. *Adv. Funct. Mater.* **2015**, *25* (7), 1043–1052.

(18) Fu, K. K.; Wang, Z.; Dai, J.; Carter, M.; Hu, L. Transient Electronics: Materials and Devices. *Chem. Mater.* **2016**, *28* (11), 3527–3539.

(19) Li, D.; Xia, Y. Electrospinning of Nanofibers: Reinventing the Wheel? *Adv. Mater.* **2004**, *16* (14), 1151–1170.

(20) Huang, C.; Soenen, S. J.; Rejman, J.; Lucas, B.; Braeckmans, K.; Demeester, J.; De Smedt, S. C. Stimuli-Responsive Electrospun Fibers and Their Applications. *Chem. Soc. Rev.* **2011**, *40* (5), 2417.

(21) Han, D.; Yu, X.; Chai, Q.; Ayres, N.; Steckl, A. J. Stimuli-Responsive Self-Immolative Polymer Nano Fi Ber Membranes Formed by Coaxial Electrospinning. **2017**.*9(13), 11858-11865*

(22) Agarwal, S.; Greiner, A.; Wendorff, J. H. Functional Materials by Electrospinning of Polymers. *Prog. Polym. Sci.* **2013**, *38* (6), 963–991.

(23) Bognitzki, M.; Czado, W.; Frese, T.; Schaper, A.; Hellwig, M.; Steinhart, M.; Greiner, A.; H. Wendorff, J. *Nanostructured Fibers Via Electrospinning*; 200, *13(1)*, 70-72.

(24) Ohlendorf, P.; Ruyack, A.; Leonardi, A.; Shi, C.; Cuppoletti, C.; Bruce, I.; Lal, A.; Ober, C. K. Transient Fiber Mats of Electrospun Poly (Propylene Carbonate) Composites with Remarkable Mechanical Strength. **2017**.*9(30)*, 25495-25505

(25) ITO,HIROSHI WILLSON, G. Chemical Amplifier in the Design of Dry Developing Resist Materials. *Polym. Eng. Sci.* **1983**, *23* (18).1012-1018

(26) Avital-Shmilovici, M.; Shabat, D. Self-Immolative Dendrimers: A Distinctive Approach to Molecular Amplification. *Soft Matter* **2010**, *6* (6), 1073.

(27) García, S. J.; Fischer, H. R.; Van Der Zwaag, S. A Critical Appraisal of the Potential of Self Healing Polymeric Coatings. *Prog. Org. Coatings* **2011**, *72* (3), 211–221.

(28) Esser-Kahn, A. P.; Sottos, N. R.; White, S. R.; Moore, J. S. Programmable Microcapsules from Self-Immolative Polymers. *J. Am. Chem. Soc.* **2010**, *132* (30), 10266–10268.

(29) Diesendruck, C. E.; Peterson, G. I.; Kulik, H. J.; Kaitz, J. a; Mar, B. D.; May, P. a; White, S. R.; Martínez, T. J.; Boydston, A. J.; Moore, J. S. Mechanically Triggered Heterolytic Unzipping of a Low-Ceiling-Temperature Polymer. *Nat. Chem.* **2014**, *6* (7), 623–628.

(30) Caruso, M. M.; Davis, D. A.; Shen, Q.; Odom, S. A.; Sottos, N. R.; White, S. R.; Moore, J. S. Mechanically-Induced Chemical Changes in Polymeric Materials. *Chem. Rev.* **2009**, *109* (11), 5755–5798.

(31) Shi, X. Y.; Tan, T. W. Preparation of Chitosan/Ethylcellulose Complex Microcapsule and Its Application in Controlled Release of Vitamin D2. *Biomaterials* **2002**, *23* (23), 4469–4473.

(32) Camera, K. L.; Wenning, B.; Lal, A.; Ober, C. K. Transient Materials from Thermally-Sensitive Polycarbonates and Polycarbonate Nanocomposites. *Polym. (United Kingdom)* **2016**, *101(2016)*, 59–66.

(33) Phillips, O.; Schwartz, J. M.; Kohl, P. A. Thermal Decomposition of Poly(Propylene Carbonate): End-Capping, Additives, and Solvent Effects. *Polym. Degrad. Stab.* **2016**, *125*, 129–139.

(34) Ma, L.; Baumgartner, R.; Zhang, Y.; Song, Z.; Cai, K.; Cheng, J. UV-Responsive Degradable Polymers Derived from 1-(4-Aminophenyl) Ethane-1,2-Diol. *J. Polym. Sci. Part A Polym. Chem.* **2015**, *53* (9), 1161–1168.

(35) Lopez Hernandez, H.; Kang, S. K.; Lee, O. P.; Hwang, S. W.; Kaitz, J. A.; Inci, B.; Park, C. W.; Chung, S.; Sottos, N. R.; Moore, J. S.; et al. Triggered Transience of Metastable Poly(Phthalaldehyde) for Transient Electronics. *Adv. Mater.* **2014**, *26* (45), 7637–7642.

(36) Fomina, N.; McFearin, C.; Sermsakdi, M.; Edigin, O.; Almutairi, A. UV and Near-IR Triggered Release from Polymeric Nanoparticles. *J. Am. Chem. Soc.* **2010**, *132* (28), 9540–

9542.

(37) Xu, J.; Liu, C.; Hsu, P. C.; Liu, K.; Zhang, R.; Liu, Y.; Cui, Y. Roll-to-Roll Transfer of Electrospun Nanofiber Film for High-Efficiency Transparent Air Filter. *Nano Lett.* **2016**, *16* (2), 1270–1275.

(38) Ohlendorf, P.; Ruyack, A.; Leonardi, A. K.; Cuppoletti, C.; Bruce, I.; Lal, A.; Ober, C. K. Transient Fiber Mats of Electrospun Poly (Propylene Carbonate) Composites with Remarkable Mechanical Strength. **2017**.*9(30)*, 25495-25505

(39) Dilauro, A. M.; Phillips, S. T. Polymer Chemistry Both in Solution and the Solid State. **2015**, *6(17)*, 3252–3258.

(40) Delbosc, N. Synthesis of Polyphthalaldehyde-Based Block Copolymers: Utilization of a Thermo-Sacri Fi Cial Segment for an Easy Access to Fine-Tuned Poly(3-Hexylthiophene) Nanostructured Films. **2016**.*49(8)*, 3001-3008

(41) Kaitz, J. A.; Diesendruck, C. E.; Moore, S. End Group Characterization of Poly(Phthalaldehyde): Surprising Discovery of a Reversible, Cationic Macrocyclization Mechanism. **2013**.*135(34)*, 12755-12761.

(42) Ma, P. X. Scaffolds for Tissue Fabrication. *Mater. Today* **2004**, *7* (5), 30–40.

(43) Schindler, C.; Williams, B. L.; Patel, H. N.; Thomas, V.; Dean, D. R. Electrospun Polycaprolactone / Polyglyconate Blends : Miscibility , Mechanical Behavior , and Degradation. *Polymer (Guildf).* **2013**, *54* (25), 6824–6833.

(44) Kruger, S. A.; Higgins, C.; Cardineau, B.; Younkin, T. R.; Brainard, R. L. Catalytic and Autocatalytic Mechanisms of Acid Amplifiers for Use in EUV Photoresists. *Chem. Mater.* **2010**, *22* (19), 5609–5616.

(45) Kruger, S.; Revuru, S.; Higgins, C.; Gibbons, S.; Freedman, D. A.; Yueh, W.; Younkin, T.

R.; Brainard, R. L. Fluorinated Acid Amplifiers for EUV Lithography. **2009**, *131(29)*9862–9863.

(46) Kancheva, M.; Toncheva, A.; Manolova, N.; Rashkov, I. Enhancing the Mechanical Properties of Electrospun Polyester Mats by Heat Treatment. *Express Polym. Lett.* **2015**, *9* (1), 49–65.

(47) Peterson, G. I.; Boydston, A. J. Kinetic Analysis of Mechanochemical Chain Scission of Linear Poly (Phthalaldehyde). **2014**, *35(18)*, 1611–1614.

(48) Lett, J. D. G. C. P.; Trent, J. S.; Scheinbeim, J. I.; Couchman, P. R. Microscopy. **1983**, *598* (2), 589–598.

(49) Saba, N.; Tahir, P. M.; Jawaid, M. A Review on Potentiality of Nano Filler/Natural Fiber Filled Polymer Hybrid Composites. *Polymers (Basel).* **2014**, *6* (8), 2247–2273.

(50) Park, J. H.; Karim, M. R.; Kim, I. K.; Cheong, I. W.; Kim, J. W.; Bae, D. G.; Cho, J. W.; Yeum, J. H. Electrospinning Fabrication and Characterization of Poly(Vinyl Alcohol)/Montmorillonite/Silver Hybrid Nanofibers for Antibacterial Applications. *Colloid Polym. Sci.* **2010**, *288* (1), 115–121.

(51) Jagur-Grodzinski, J. Nanostructured Polyolefins / Clay Composites : Role of the Molecular Interaction at the Interface. *Polym. Adv. Technol.* **2006**, *17* (April), 395–418.

(52) Yeo, L. Y.; Friend, J. R. Electrospinning Carbon Nanotube Polymer Composite Nanofibers. *J. Exp. Nanosci.* **2006**, *1* (2), 177–209.

(53) Sen, R.; Zhao, B.; Perea, D.; Itkis, M. E.; Hu, H.; Love, J.; Bekyarova, E.; Haddon, R. C. Preparation of Single-Walled Carbon Nanotube Reinforced Polystyrene and Polyurethane Nanofibers and Membranes by Electrospinning. *Nano Lett.* **2004**, *4* (3), 459–464.

(54) Li, L.; Bellan, L. M.; Craighead, H. G.; Frey, M. W. Formation and Properties of Nylon-6

and Nylon-6/Montmorillonite Composite Nanofibers. *Polymer (Guildf).* **2006**, *47* (17), 6208–6217.

(55) Pan, H.; Li, L.; Hu, L.; Cui, X. Continuous Aligned Polymer Fibers Produced by a Modified Electrospinning Method. *Polymer (Guildf).* **2006**, *47* (14), 4901–4904.

(56) Huang, C.; Chen, S.; Reneker, D. H.; Lai, C.; Hou, H. High-Strength Mats from Electrospun Poly(p-Phenylene Biphenyltetracarboximide) Nanofibers. *Adv. Mater.* **2006**, *18* (5), 668–671.